ESTCP

FINAL REPORT

Demonstration and Validation of the Seismic-Acoustic Impact Monitoring and Assessment (SAIMA) System

Kevin Hutchenson
Ray Conner
Christopher Bailey
Quantum Technology Sciences

Janet Simms
USACE-ERDC Vicksburg

Buddy Leavell
Ft. Sill

Annette Butler
USACE-Huntsville

June 2017

ESTCP Project MR-201419

REPORT DOCUMENTATION PAGE

Form Approved
OMB No. 0704-0188

1. REPORT DATE *(DD-MM-YYYY)*	2. REPORT TYPE	3. DATES COVERED *(From - To)*
04-21-2017	ESTCP Final Report	6/24/2014 - 6/24/2017

4. TITLE AND SUBTITLE

Demonstration and Validation of the Seismic-Acoustic Impact Monitoring and Assessment (SAIMA) System

5a. CONTRACT NUMBER
W912HQ-14-C-0040

5b. GRANT NUMBER

5c. PROGRAM ELEMENT NUMBER

6. AUTHOR(S)

Quantum Technology Sciences: Kevin Hutchenson, Ray Conner & Christopher Bailey
USACE-ERDC Vicksburg: Janet Simms
Ft. Sill: Buddy Leavell
USACE-Huntsville: Annette Butler

5d. PROJECT NUMBER
MR-201419

5e. TASK NUMBER

5f. WORK UNIT NUMBER

7. PERFORMING ORGANIZATION NAME(S) AND ADDRESS(ES)

Quantum Technology Sciences, Inc
1980 North Atlantic Ave, Suite 201
Cocoa Beach, Florida 32931

8. PERFORMING ORGANIZATION REPORT NUMBER

MR-201419

9. SPONSORING / MONITORING AGENCY NAME(S) AND ADDRESS(ES)

ESTCP Program Office
4800 Mark Center Drive, Suite 17D08
Alexandria, VA 22350-3600

10. SPONSOR/MONITOR'S ACRONYM(S)
ESTCP

11. SPONSOR/MONITOR'S REPORT NUMBER(S) MR-201419

12. DISTRIBUTION / AVAILABILITY STATEMENT

DISTRIBUTION STATEMENT A. Approved for public release: distribution unlimited.

13. SUPPLEMENTARY NOTES

14. ABSTRACT

The purpose of this project is to demonstrate and validate the Seismic Acoustic Impact Monitoring Assessment (SAIMA) system capabilities to detect, classify, locate, and report in near real-time artillery Unexploded Ordnance (UXO) and Low-Order Ordnance Detonations (LOD) events, as well as High-Order Detonation (HOD) events. This system will provide added value knowledge for Explosive Ordnance Disposal (EOD) personnel and environmental sampling teams of where to find UXO rounds and newly deposited Munition Constituents (MC) from LOD events. With immediate knowledge of individual UXO round locations will make prompt cleanup of these rounds possible, removing UXO rounds sooner will reduce the likelihood those rounds will be ruptured by subsequent detonations, thus reducing the incidence of MC deposits.

15. SUBJECT TERMS
Seismic-acoustic sensors, artillery, UXO, LOD, HE detection, location, MC cleanup, removal,

16. SECURITY CLASSIFICATION OF:			17. LIMITATION OF ABSTRACT	18. NUMBER OF PAGES	19a. NAME OF RESPONSIBLE PERSON
a. REPORT	b. ABSTRACT	c. THIS PAGE			Ray Conner
UNCLASSIFIED	UNCLASSIFIED	UNCLASSIFIED	SAR	60	19b. TELEPHONE NUMBER *(include area code)* 321-784-0048 x 116

FINAL REPORT
Project: MR-201419

TABLE OF CONTENTS

TABLE OF CONTENTS (Continued)

Page

LIST OF FIGURES

Page

LIST OF FIGURES

Page

LIST OF TABLES

Page

ACRONYMS AND ABBREVIATIONS

AIC	Akaike Information Criteria
APG	Aberdeen Proving Ground
ARF	Array Response Function
ATS	Advanced Technology Site
BRAC	Base Realignment and Closure
CCAFS	Cape Canaveral Air Force Station
CTBTO	Comprehensive Nuclear Test Ban Treaty Organization
DoD	Department of Defense
EOD	Explosive Ordnance Disposal
ERDC	Engineering Research and Development Center
ESTCP	Environment Security Technology Certification Program
FK	Frequency Wavenumber
FL	Florida
FOUO	For Official Use Only
ft	Foot, feet
FUDS	Formerly Used Defense Sites
GPS	Global Positioning System
HE	High Energy
HOD	High-order Ordnance Detonation
Hz	Hertz
IDC	International Data Center
ITD	Impulsive Transient Detection
LDA	Linear Discriminant Analysis
LTA	Long Term Average
LOD	Low-order Ordnance Detonation
m	meters
MC	Munition Constituents
MEL	Multiple Event Location
QTSI	Quantum Technology Sciences, Inc
RDPS	Remote Data Processing Station
SADAR	Seismic-Acoustic Detection and Ranging

SAIMA	Seismic-Acoustic Impact Monitoring and Assessment
sec	second
SNR	Signal-To-Noise Ratio
SEL	Single Event Location
SERDP	Strategic Environmental Research and Development Program
STA	Short Term Average
USNDC	United States National Data Center
UTC	Universal Coordinated Time
UXO	Unexploded Ordnance

1.0 INTRODUCTION

1.1 BACKGROUND

Significant concern exists over the release of Munitions Constituents (MC) on Department of Defense (DoD) training and testing ranges, and the potential for MC to migrate off the range areas. The largest source of MC is Low-Order Ordnance Detonations (LOD) and Unexploded Ordnance (UXO) rounds that are ruptured by other detonations (SERDP, 2007). Therefore, locating individual UXO and LOD impacts as they occur would help identify MC source terms so effects can be proactively mitigated.

The Seismic-Acoustic Impact Monitoring and Assessment (SAIMA) System is designed to detect, locate, and classify UXO, LOD, and High Explosive (HE) impacts on artillery training and testing ranges. During its development, several sites were visited to test and demonstrate the developing technology. Sites discussed in this report include: Aberdeen Proving Ground (APG), MD; Ft. Sill, Lawton, OK; and the Advanced Technology Site (ATS), CCAFS, FL, for testing.

1.2 OBJECTIVE OF THE DEMONSTRATION

The objective of this demonstration is to collect UXO (duds) and Fire for Effect data and validate SAIMA capability to automatically detect, classify, and locate UXO and LOD impacts on range.

1.3 REGULATORY DRIVERS

The demonstration site for the data collect was conducted at the North Arbuckle Range, Ft. Sill, Oklahoma in October 2016. However, prior collects are important and are included in the report to aid in the evaluation.

1.4 ACKNOWLEDGEMENTS

Janet Simms, and Jay Bennett from ERDC, was onsite during the installation and collect phases of the project. They consulted with Ft. Sill Range Control and supported the logistics for range access to obtain the data needed for the analysis and demonstration.

2.0 TECHNOLOGY

This section provides an overview of the Seismic-Acoustic Impact Monitoring and Assessment (SAIMA) system developed to detect and locate unexploded ordinance (UXO) and low-order detonations (LOD) on artillery training and testing ranges.

2.1 TECHNOLOGY DESCRIPTION

The SAIMA system consists of a network of seismic-acoustic sensors distributed around an impact range (Figure 1). Each station consists of an array of sensors connecting to a node that processes the signal and transmits the data to a Remote Data Processing Station for display. The number of arrays deployed around the range depends on the size of the range and munitions being detected. A trigger sensor is located near the firing station to detect the muzzle blast and firing times of the munitions.

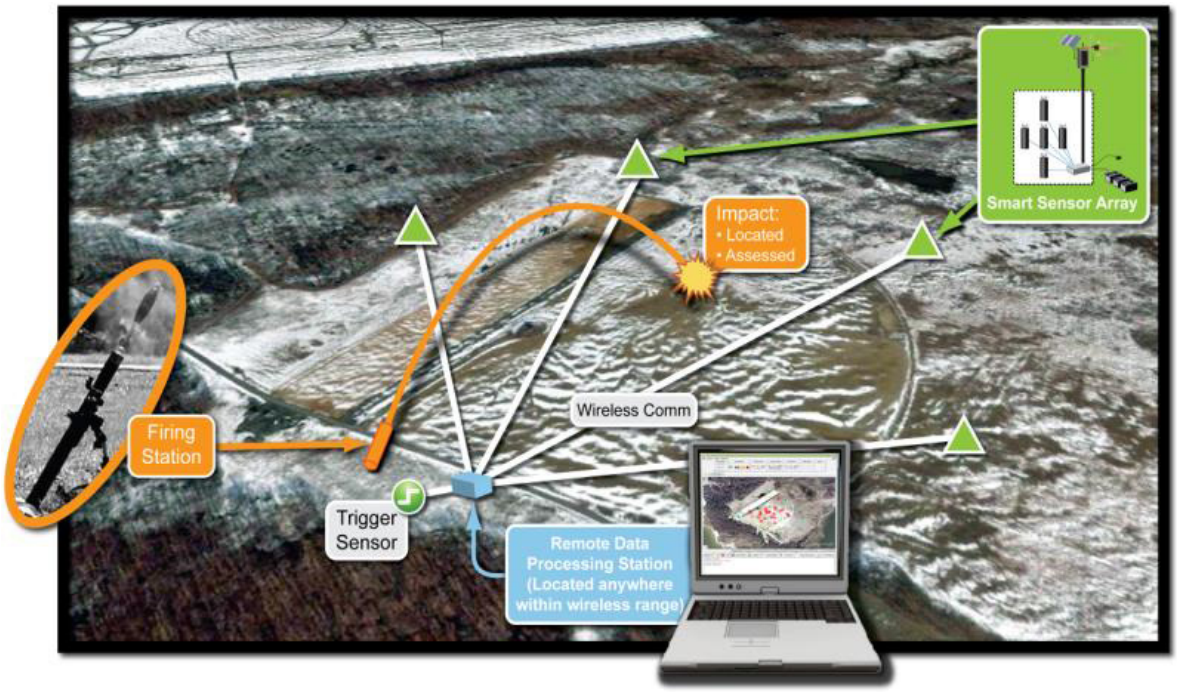

Figure 1. An Example SAIMA Deployment Around an Impact Range.

Seismic-acoustic sensors are buried in shallow holes around the monitored area in a two-dimensional array pattern capable of sensing both seismic and acoustic energy of the munitions impact and detonation. The array design provides an azimuthal direction of the arrival signal that can be associated with multiple arrays by beam crossing and geo-locating the energy source.

2.2 TECHNOLOGY DEVELOPMENT

With the Department of Defense (DoD) using over two million HE munitions per year and a significant fraction as UXO, reducing costly range remediation and environmental restoration efforts will offer significant savings. The SAIMA approach offers a solution where UXO and LOD rounds are detected and located as they occur so cleanup can be a proactive part of routine range management.

This preventative approach, once implemented DoD-wide, would stop the buildup of additional UXO for cleanup under Base Realignment and Closure (BRAC) and Formerly Used Defense Sites (FUDS) programs, and make achieving cleanup goals actually feasible.

The SAIMA system employs a set of sophisticated signal processing algorithms to detect, classify, and locate ordnance impacts in near real-time. These algorithms were developed by Quantum engineers and scientists from concepts in the areas of seismology, applied geophysics, and statistical analysis.

Impulsive Transient Detection (ITD) Algorithm. The ITD algorithm is designed to detect impulsive signals in time-series that are created from physical sources, and is similar to other "auto-pickers" used in seismology (e.g., Diehl *et al.*, 2009). The ITD is responsible for the detection of seismic and acoustic phases from UXO and HE events, and operates only during periods when an impact event is anticipated. This "anticipation" is accomplished with a synchronized trigger sensor, which upon detecting a gun/mortar at the firing point alerts the ITD to the impending event, and creates a detection "window" (time segment of the waveform) based on a theoretical time of impact within which the ITD operates. The ITD employs a short-term averaging/long-term averaging (STA/LTA) signal-to-noise ratio (SNR) technique. The STA is sensitive to a rapid increase in amplitude in the time series, whereas the LTA measures the noise, interference, and clutter background in the time series. The ratio of the two becomes an estimate of the local SNR. A detection is declared when the ratio exceeds a threshold, T. The STA/LTA detection is then passed to an Akaike Information Criterion (AIC) algorithm (Akaike, 1974), which automatically pinpoints a more accurate arrival and cessation time for the detection. The most basic form of the AIC is expressed in terms of the time series and a pre-determined distribution of the generating process, which for the SAIMA system is a normal distribution of background noise. The ITD delineates the area of the time series that contains the signal of interest by creating a detection object. This object is passed to the FK algorithm for further processing.

Frequency-Wavenumber (FK) Analysis. FK analysis is an array processing technique used to determine an optimal azimuth (and slowness, which is inverse speed) from an array to a coherent signal source (Smart and Flinn, 1971). Windowed waveforms, with the length depending on distance, from all array elements are used to construct a beam at each azimuth and slowness point of a slowness area (grid spacing). A beam is formed by a time shift corresponding to the slowness and azimuth at each grid point. The optimal signal azimuth and slowness values are determined by the beam with the most power, usually correlated with the largest F-statistic (or coherency). The exact location (latitude, longitude) of each sensing element (which is measured from an array-central GPS point) is needed as a common time base for all sensing elements of the array. Spatial resolution can be enhanced by using more grid points; some coherent noise may be removed if outside the frequency band by filtering the waveforms before the FK process. The largest coherent signal with the associated azimuth and slowness is used to form the beam. A graphical depiction of the FK results from a small time window is shown in Figure 2.

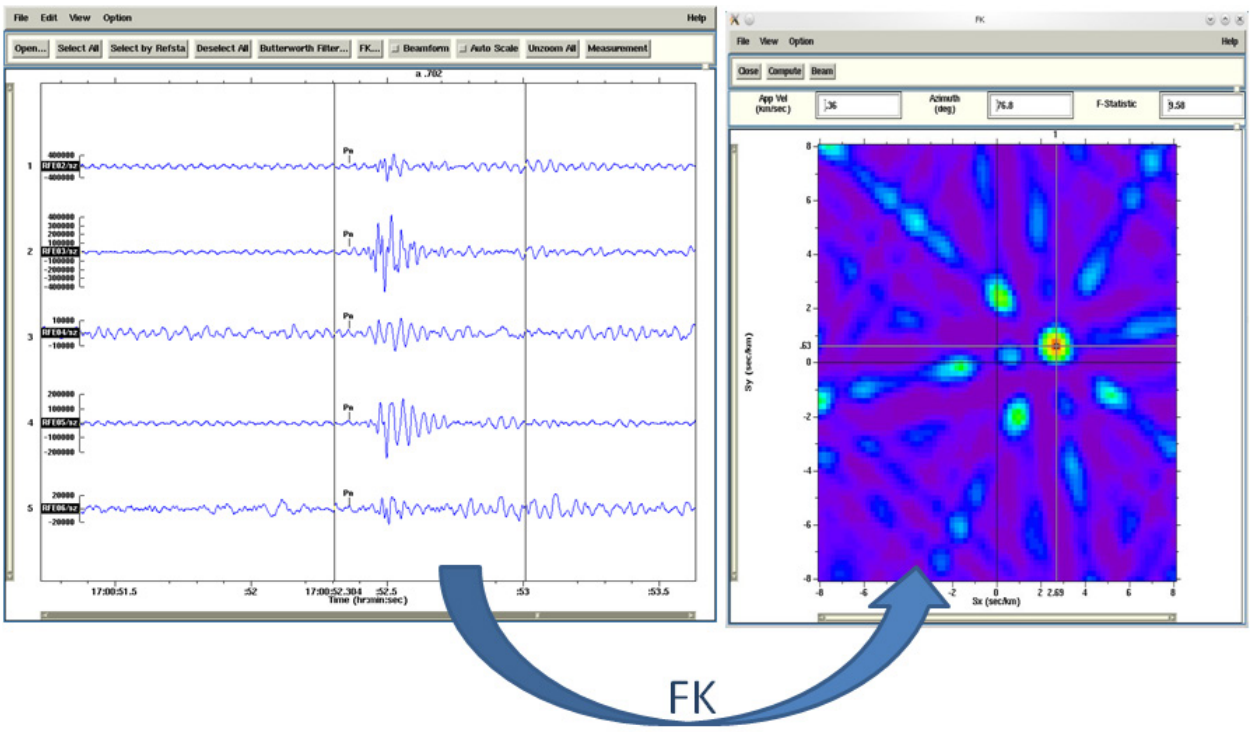

Figure 2. An Example Waveform Segment from the Time Domain and Resulting FK.

Impulsive Transient/Cluster Feature Extractor. This method takes in raw continuous data (or beamed data) and derived information in the form of discrete single-cell detections and performs three major tasks: 1) cluster agglomeration; 2) time segment retrieval; and 3) feature extraction. The output is in the form of discrete cluster objects composed of detections representing the entire detected impulse objects and containing features derived from the entire time span (VanDeMark *et al.*, 2013, 2010, 2009).

Impulsive Transient Phase Associator. This associator operates on cluster objects and determines if they are a signal of interest. The associator accomplishes this through *a priori* knowledge of station geometry and phase velocities. Simplistically, the associator looks for a set of incoming phases from all stations within a predefined time association window given the assumption that the origin of the signal is somewhere within the impact area. The derived features from these associated clusters are then forwarded to the location and classification algorithms for further processing (VanDeMark *et al.,* 2013, 2010, 2009).

Event Location. Array processing event location is achieved via a staged crossed beam and subsequent travel time inversion. The SAIMA system uses multiple approaches to calculate location solutions for all mortar and artillery impacts. The first step is a "crossed beam" approach using results from array processing. From the azimuthal direction from the station to the detected and beamed event determined from the FK, the location where all beams cross is the approximate event location (Figure 3). This solution provides a seed location for an inversion routine to calculate a "better" location solution of each impact using a single event location (SEL) algorithm (Lay and Wallace, 1995). If necessary and with sufficient data, this solution could be replaced or supplemented by relocation of the event using a master event location (MEL) algorithm.

Details of this MEL technique are fully detailed in Erickson *et al.* (2003a, 2003b) and VanDeMark et al. (2010). To increase the location accuracy, the SAIMA system can also use a Master Event Correction file derived from specific calibration points (accomplished when the system is installed) that help reduce the location bias.

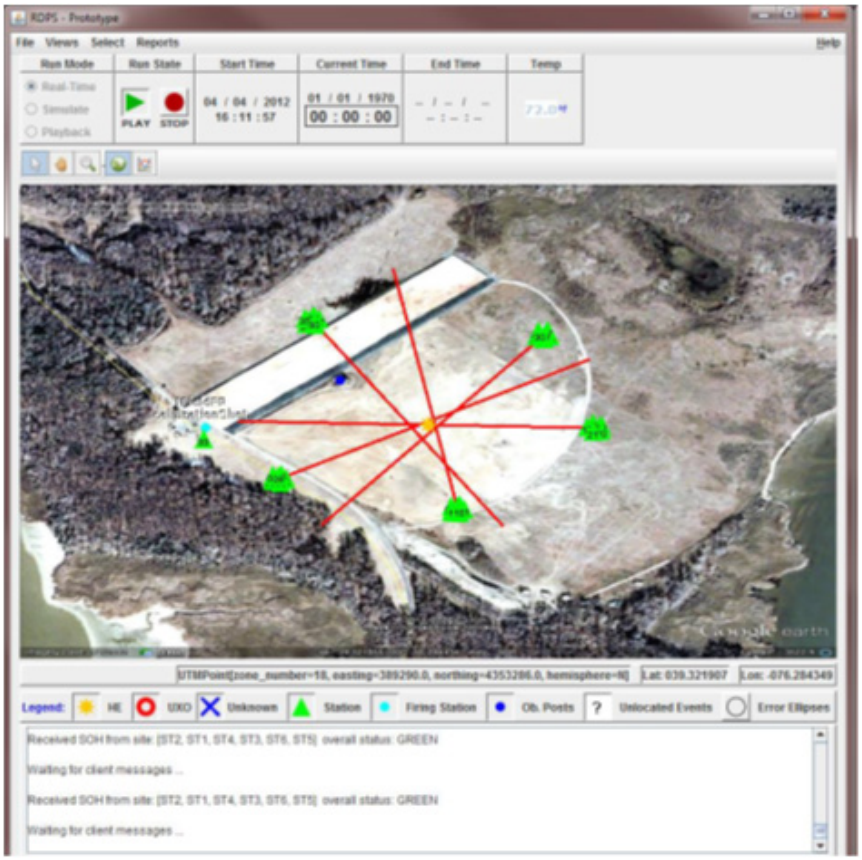

Figure 3. An Example SAIMA Display of Event Location.

Event Classification. This is accomplished using several features. The SAIMA system uses a linear discrimination analysis (LDA) (Fisher, 1936; Hastie et al., 2009) classification architecture to determine if an unknown event is either HE or UXO. The classification features used for SAIMA are mean signal energy of the seismic phase, phase ratio between the seismic and acoustic phases, and their spectral ratio (VanDeMark *et al.*, 2009). A training set of known event types, initially obtained from each range, is used to obtain measurement parameter estimates for each event type. Subsequently, the probability that the unknown event being processed is a member of either of the two known event types is calculated and the classification decision is made. The probability is calculated as: $P(x \mid type) = (x - \mu_{type})^T C_P^{-1} (x - \mu_{type})$, where x is the unknown event, μ_{type} is the mean of the training data by type, and C_P^{-1} is the inverse of the pooled covariance matrix of the training data (Hastie *et al.*, 2009).

A field deployment at Ft. Sill, Oklahoma, in summer 2012 demonstrated acoustic locations at a large range (QTSI, 2013). Recent systems tests with five arrays using a synthetic UXO source (impact source only; no acoustic phases) at APG in November 2012 (80 m by 80 m) resolved locations within 0.5 m of ground truth with coverage ellipses at 0.1 m^2 (using time and azimuth).

Assuming upward linear scaling to a larger impact area (3.2 km by 3.2 km), calculated locations would be within 2.5–3m of ground truth with coverage ellipses on the order of 3–4 m^2. In practice, a second field deployment at APG in yielded average locations of inert rounds within 4 m (ignoring a few errant solutions), and spotter rounds were located within 2 m (Hutchenson *et al.,* 2015, 2013).

A complete functional SAIMA prototype was installed at Ft. Sill in late summer 2013 consisting of five (5) 8 seismic-acoustic sensor arrays, one (1) trigger sensor, and a remote data processing station communicating between sites via 900 MHz radio. The tests successfully demonstrated the detection and localization of 105 mm and 155 mm impacts at the North Arbuckle Range (Figure 4).

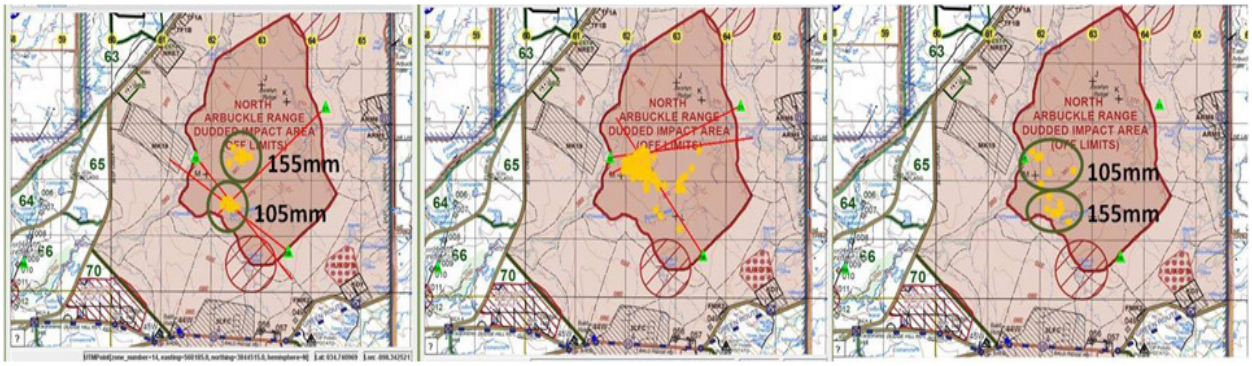

Figure 4. SAIMA Demonstration Detecting and Locating Artillery Impacts.

Quantum technology has significantly improved since deployment of SAIMA in 2013, particularly in development of the seismic-acoustic sensor. This new hardware (Figure 5) was used at Ft. Sill in October 2016 to collect and analyze UXO (inert rounds) and Fire for Effect impacts on range. The new sensor proved to be more sensitive than the original deployed prototype sensor in detecting and locating 155 mm inert rounds (UXO). The new hardware has also undergone long-term system reliability tests and is built to meet the Environmental MIL-STD-810 design and test limits (QTSI, 2015).

Figure 5. New Seismic-acoustic Sensor and Hardware Technology.

2.3 ADVANTAGES AND LIMITATIONS OF THE TECHNOLOGY

This system will provide added value knowledge for EOD personnel and environmental sampling teams to find UXO rounds and newly deposited MC from LOD events. Since immediate knowledge of individual UXO round locations will make prompt cleanup of these rounds possible, removing UXO rounds sooner will reduce the likelihood those rounds will be ruptured by subsequent detonations, thus reducing the incidence of MC deposits. Also, when prompt cleanup is not possible, environmental managers can use the knowledge of UXO and LOD impact locations to forecast the fate of MC and assess the risks of surface and ground water contamination.

2.3.1 Advantages

- Detect and localize UXO (inert/dud), LOD, and HOD impacts in near-real time
- Reduce UXO/MC cleanup and remediation efforts
- Long term cost and environmental benefits

2.3.2 Limitations

The effectiveness of the seismic/acoustic system at the various sites is highly dependent upon these factors:

- Source strength: The distance between sensors and impact area will determine the ability to detect and locate the source. The larger munitions (e.g. 105 mm and 155 mm) impacts will be easier to detect and locate. Additional sensors may need to be deployed within the impact area to detect and locate smaller UXO munitions (e.g. 60 mm or 81 mm caliber mortars).

- Seismic and acoustic propagation characteristics: Seismic wave propagation is highly dependent upon the type of geologic material present at the range. Changes in temperature and wind speeds will also influence the seismic and acoustic propagation characteristics.

- Seismic and acoustic background noise levels: High surface winds can increase both seismic and acoustic noise levels. Other natural and manmade noise sources can reduce the sensitivity and detection range of the system.

3.0 PERFORMANCE OBJECTIVES

The performance objectives for the Phase I ESTCP work can be summarized (Table 1). At the time of submittal, the probability of success to meet these objectives was high. The plan was to immediately transition from one effort to the ESTCP effort.

A later section summarizes the key performance results against the objectives.

Table 1. ESTCP Phase I Performance Objectives.

Performance Objective	Metric	Data Required	Success Criteria
Quantitative Performance Objectives			
Assess SAIMA system currently deployed at Ft Sill.	Number of working: • Nodes • Sensors • Radios • Battery power • Solar panels.	• Recorded data from nodes. • Sensor performance • Radio performance • Power measurements	The system can be restored to operational state for follow-on data collections.
Collect and analyze data for UXO detections.	Seismic P-waves (kinetic energy) detected from UXO impacts.	• Recorded data from SAIMA system. • Ground truth location of UXO (inert) impacts	Analyze P-waves from recorded data and determine location of UXO impact within TBD meters of ground truth.
Collect and analyze "fire for effect" for single dud detections.	Single dud (UXO) impact detected among live rounds.	• Recorded data from SAIMA system. • Ground truth location of duds.	Discern and locate single dud detections among live rounds.

4.0 SITE DESCRIPTION

Several sites were worked during this effort. Two main sites were utilized to demonstrate and test the effectiveness of the SAIMA hardware and software. While Aberdeen Proving Grounds (APG) was worked in a BAA effort just prior to the current ESTCP program, the results are directly related and relevant to the current program. Under the ESTCP program, the North Arbuckle Range was the main field of effort for the ESTCP efforts. Both are described in this section.

This section describes each site, the history of use, the geology, and the munitions contamination.

4.1 ABERDEEN PROVING GROUND, MARYLAND

APG is located on the Chesapeake Bay, approximately 25 km northeast of Baltimore, Maryland. It lies within the Coastal Plain Province, one of Maryland's five distinct physiographic provinces. The province is underlain by a wedge of unconsolidated sediments consisting of gravel silt, sand, and clay dipping gently eastward and thickening as it approaches the Atlantic coastline, and ranges in age from Triassic to Quaternary (Edwards, 1981).

Previous seismic refraction studies in the Canal and Lauderick Creek areas of APG illuminated two distinct seismic velocity layers (McGinnis *et al.*, 1992; Sharp *et al.*, 1999): a top layer with a compressional wave seismic velocity of ~800 m/s, generally interpreted as Quaternary aged unconsolidated and unsaturated silt, clay, and sand; and an underlying layer with a compressional wave seismic velocity of 2,000 m/s, which is generally interpreted as consolidated and saturated Cretaceous aged clay-sand and clean saturated sands. Both of these study areas are in the northern part of the range.

The I-Field site (Figure 6), located near the southern part of the peninsula, was utilized for the development effort under this program. This is an inert field, only non-exploding ordinance are fired into the field. All ordinances are recovered. The top soil layer at the array sites surrounding the range area was physically interpreted as partially saturated, clay-sand. A refraction analysis undertaken in 2008 provided a simple layer over a half space at the I-Field site (VanDeMark *et al.*, 2013, 2009) with the half space velocity at approximately 1540 m/s.

Figure 6. Map View and Range View (US Army, 2011) for the I-Field range, APG, MD.

The impact area is easily discernible in the map image.

While the field is relatively small, only 540 m by 365 m, it is an inert field; there is no contamination from UXO or cratering from HE. The surface is routinely broken up to keep soft for munitions recovery and to lessen damage to the inert munitions. This allows a precise measurement of the munitions position using GPS and a direct comparison with the calculated results.

4.2 NORTH ARBUCKLE RANGE, FT. SILL, LAWTON, OKLAHOMA

Ft. Sill is located at Lawton, OK, just east of the Wichita Mountains in southern Oklahoma. The Wichita Mountains are a series of Cambrian (and possibly Proterozoic) igneous knobs and Cambrian to Ordovician sedimentary hills protruding through the Permian shaly plains with topographic relief on the order of 335-396 m (1,100-1,300 ft) (Gilbert, 1982).

Of the several ranges present, the collects have occurred using the North Arbuckle Range, northeast of Lawton and east of I-44 (Figure 7). The North and South Arbuckle Ranges are east of the topographic highs of the Wichita Mountains. The North Arbuckle Range is fairly flat, consisting of low, rolling hills cut by small stream valleys. An observation post (OP), a tower at the southern end of the North Arbuckle Range, is located on the southwest corner of the field (Figure 7).

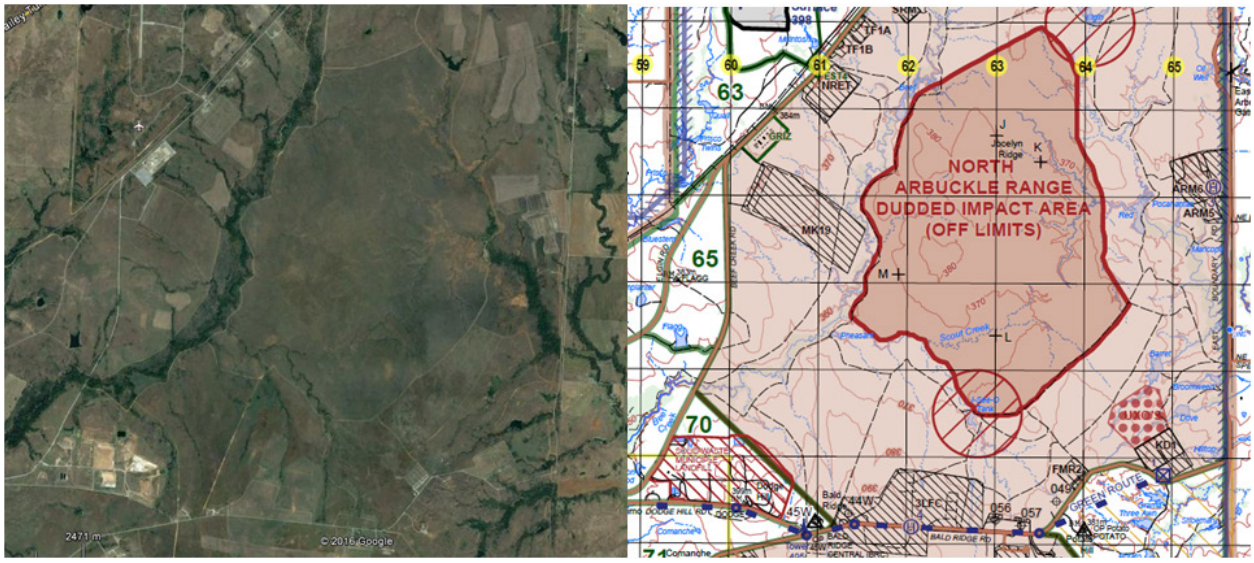

Figure 7. Map View and Range View (US Army, 2011) for the North Arbuckle Range, Ft. Sill, OK.

The impact area is easily discernible in the map image.

This is an active field, receiving 155 mm and 105 mm artillery and is host for a number of small arms fields surrounding the perimeter of the impact area. The field is cratered from the numerous HE and contains UXO. The impact area boundary (thick red line) is typically kept as a firebreak. During the deployments, several craters, numerous fragments, and a few UXO were discovered in the firebreak area and outside the designated impact area, indicating there are impacts beyond the marked boundaries.

5.0 TEST DESIGN

This section describes the key technologies inherent in the SAIMA system. An overview of the technology development of the system is described in an earlier section.

5.1 CONCEPTUAL EXPERIMENTAL DESIGN

Each of the SAIMA sites consist of a node, eight (8) sensors, cables, GPS antennae, batteries, power cable, and 900 MHz radio. The many installed nodes are augmented at a central site containing a laptop and base radio. All signals are received and aggregated on the laptop.

The array is designed to capture the energy from the expected seismic-acoustic sources for a frequency band of interest; the array design is tested prior to departure. A number of designs may be attempted to vary the sensor placement, number of rings, etc. It is best with an initial estimate of surface velocity and propagation speeds of the anticipated signals. In the case of the Ft. Sill area, a prior refraction surface yielded some estimates of the surface velocity (QTSI, 2012) for seismic Rayleigh (Rg) waves. But, the acoustic wave is also a viable phase for the HE events.

The final design consisted of an eight (8) sensor array, deployed as two rings. The rings consisted of three and five sensors (Figure 8). The response of an array to incoming signals can be estimated by the array response function (ARF), calculated as (Schweitzer *et al.,* 2012; Rost and Thomas, 2009):

$$|A(\boldsymbol{k} - \boldsymbol{k}_0)|^2 = \left| \frac{1}{M} \sum_{j=1}^{M} e^{(2\pi i(\boldsymbol{k} - \boldsymbol{k}_0))\boldsymbol{r}_j} \right|^2$$

where $\boldsymbol{k}$ is the wavenumber vector of the incoming energy, $\boldsymbol{k}_0$ is the reference wavenumber vector, $\boldsymbol{r}_j$ the sensor location vectors, and M the number of sensors within the array.

The calculated response function from this design is shown with both a seismic (650 m/sec) and acoustic velocity (340 m/sec) of a wave arriving from an azimuth of 225º at 50 Hz (Figure 9). Note that different velocities and frequencies change this view. A suite of both are tested for each design.

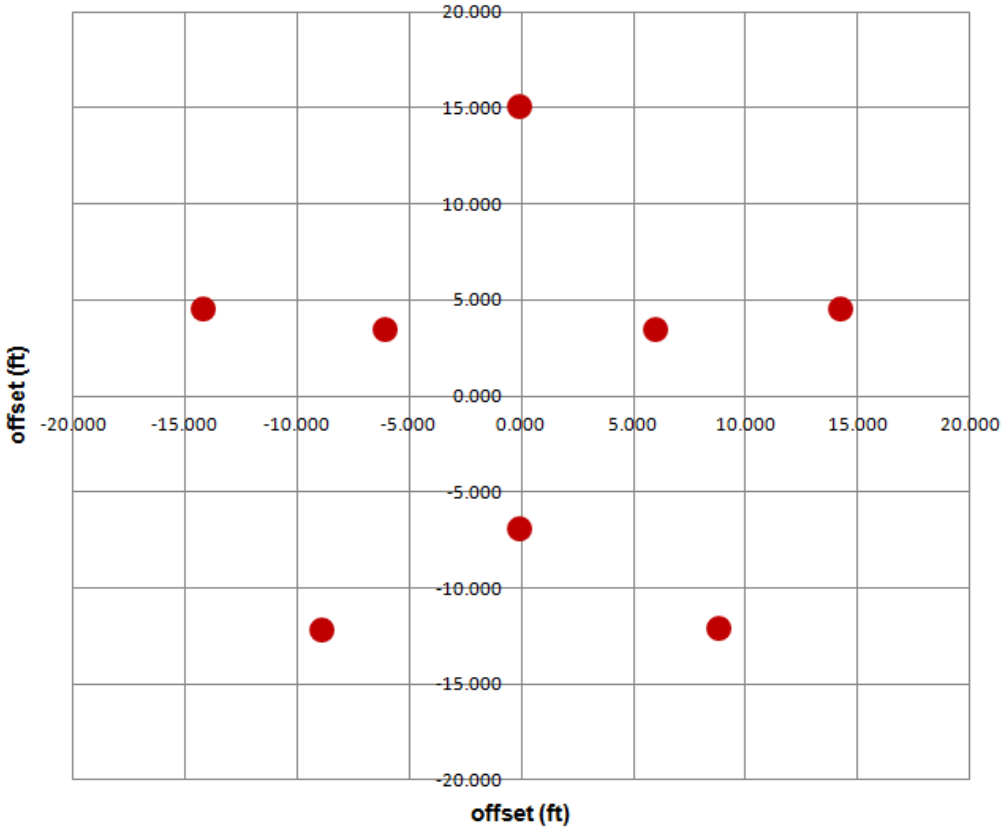

Figure 8. The Two-ring, Eight-sensor Design Deployed at Both APG and Ft. Sill.

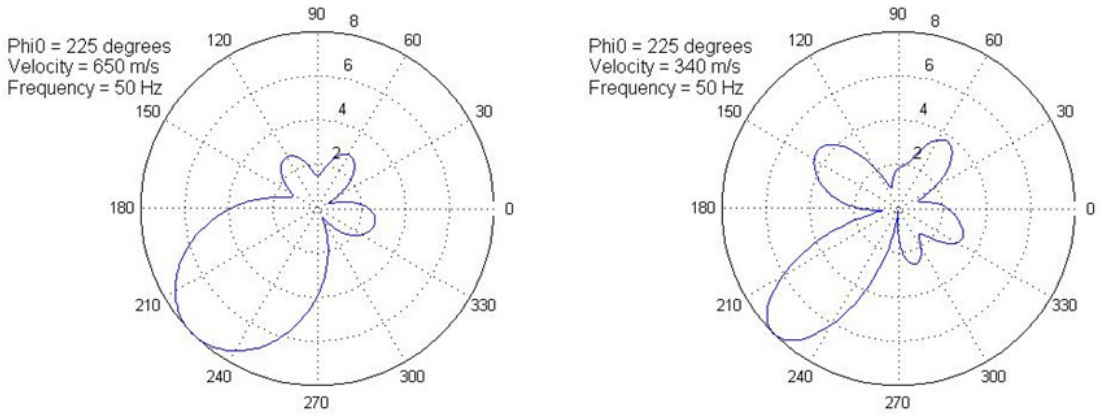

Figure 9. ARF from the Eight-sensor Design Using Both a Seismic (Left) and Acoustic (Right) Velocity at 50 Hz.

The wave is arriving from the southwest (225°).

5.2 SITE PREPARATION

Little, if any site preparation is needed in the deployment of a typical SAIMA system. In all cases, whether APG or Ft. Sill, a rough site location is determined using a map or photo (i.e. Google Earth). A final check is performed on the ground during the deployment. An initial location may shift for any number of reasons, e.g., tree growth since the last photograph, unseen wires or cables, an EOD team designates a buried object. Usually the final site location is within a few meters of the original site location.

The sensor locations for the array are measured and marked according to plan. Sensor holes are typically dug with hand tools (post-hole digger or shovel). All cables may be buried in shallow trenches if a long deployment or left on the surface if short.

5.3 SYSTEM SPECIFICATION

The SAIMA system is composed of a number of 8-element seismic-acoustic sensor arrays. The seismic-acoustic sensors are coherent as a group, and individually buried in a pattern to maximize the coverage for the ground velocities and frequencies of interest. The arrays are spaced around the impact area with respect to azimuth. The elements of the array are connected to a Node for onsite conversion to a data stream (CD1.1 format). Additionally, a Node and sensor located near each firing point is used to detect the trigger time of the weapon firing. Each Node has a GPS for position and timing, provides power management to the node and sensors, data storage, triggered data, and communicates to a Remote Data Processing Station (RDPS) via a wireless network. The RDPS (*i.e.*, laptop) receives data from all Nodes, processes the data, and displays the data to the operator on a graphic interface or a report (Figure 10).

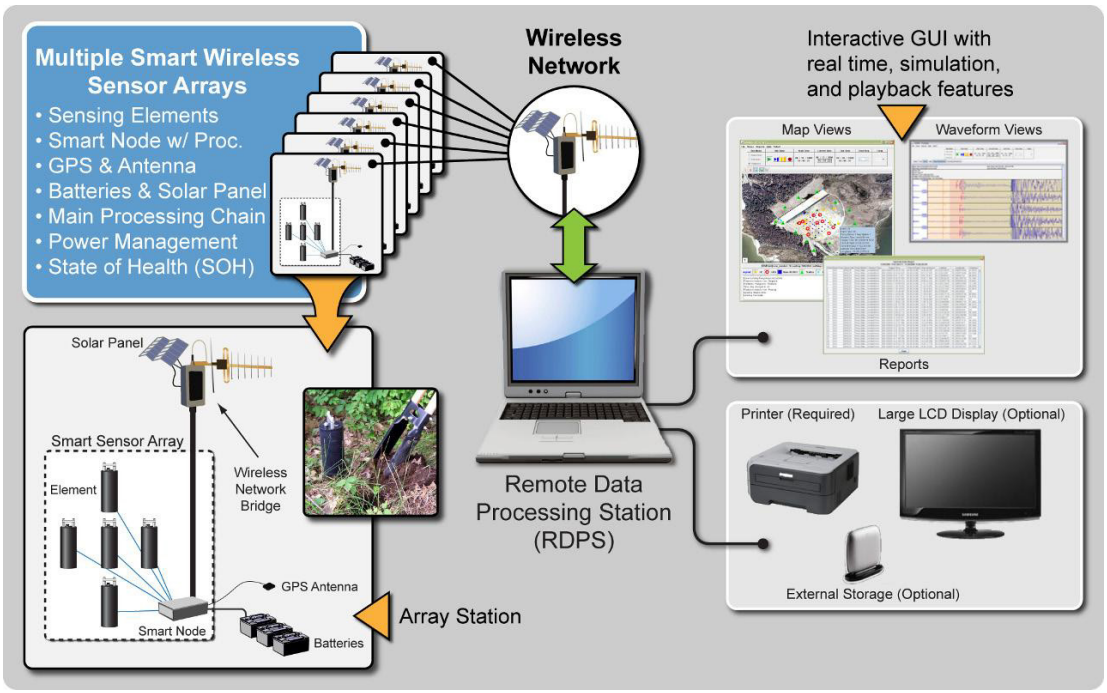

Figure 10. Overview of the SAIMA System Components.

Sensor Element. The sensor element consists of materials required to sense seismic-acoustic data, and electronic circuitry to process and interface to the node. The housing is designed to be robust under a variety of environmental conditions. When buried in a shallow hole and covered with packed dirt, the sensing element acquires the initial geophysical signal and produces continuous analog data that is transmitted to the Node for further processing.

Smart Node. The smart node receives signal data and creates digital samples synchronizing data from each of the sensor elements. The sampled data are then conditioned and provided to subsequent beam analysis steps. The beamformed data are operated upon according to a set of specific algorithms that produce detections, classifications, and localization estimates. Classifications and their associated features are transmitted to the RDPS for display.

Remote Data Processing Station (RDPS). The RDPS receives data from one or more smart nodes. The RDPS is an application which runs on a computer (*i.e.*, laptop) to receive and process information from multiple smart nodes, to associate, classify, and locate targets, generate alerts, provide state-of-health and display information and results on a graphic user interface.

5.4 CALIBRATION ACTIVITIES

When installing an array according to plan, care is taken to place the sensors in the precise pattern, within a few inches. Spatial processing algorithms need the correct placement of the sensors.

While the sensors are omni-directional, the orientation of the array is important. Typically, several impulses are performed at locations 8 m (approximately 25 ft) to the north and east of the array to check the accuracy of the array orientation. Software can correct for a few degrees, but major errors are typically caught during this step.

All sensors are checked for relative coherence prior to deployment. No sensor level calibration is needed in the field.

5.5 DATA COLLECTION

Data collection begins when the unit is powered. Typically, batteries, perhaps supplemented by a solar panel, provide continuous power for the units. More recently, units have been configured to run from Power Over Ethernet (POE).

In a typically scenario, the units are activated by a trigger node. The trigger node sends a signal via radio to the RDPS (laptop); the RDPS, in turn, sends a signal to all nodes to record and process a segment. The trigger node is activated by the firing of a gun (mortar tube or artillery). The wait period and signal segment to process are controlled via parameters.

The nodes process the data segment, detect and refine the phase(s) arrival, then send the information to the RDPS. The RDPS software combines all node information to process and report the location and type of event (UXO, LOD, or HE).

The system automatically works, with power supplied by the batteries, until the collect is over and the units are shut down. Data collects to date have run from a few days to a week.

5.6 VALIDATION

The validation of the system has been an evolving process.

The hardware has evolved over the years. The current hardware has been tested using MIL-STD-810g (QTSI, 2015); it is very hardy. Continued work improves aspects of the system.

The validation of the system software and processing algorithms has taken place in different locations and at different scales.

One of our test locations was a mere 80 m by 80 m (262 ft by 262 ft). The sources were a 3 lb. hammer hitting the ground. Locations were within 0.5 m or less with coverage ellipses on the order of 0.1 m^2 (Hutchenson *et al.,* 2015, 2013).

The APG collect was on a larger scale. The impact field was 365 m by 480 m (1197 ft by 1575 ft). As an inert field, each of the mortars could be accurately located using GPS. These results are discussed in a later section.

The Ft. Sill, North Arbuckle Range, is an active range. Limited access was provided to the inner part of the range. None of the impacts were checked using GPS. Our best check on location was via optical azimuths using orthogonally located cameras. These results are discussed in a later section.

6.0 DATA ANALYSIS AND PRODUCTS

Numerous collects have taken place to build, develop, and test the SAIMA technology. Ft. Sill has been visited under several prior contracts since 2012, and APG was visited in 2012. We have a development field on nearby CCAFS where the systems, both hardware and software, can be tested.

The technology of the SAIMA system is described in Section 2.0 with results from several collects shown in Section 7.

For the purposes of the final collect for the ESTCP effort in October 2016, the SAIMA system was not used. All processing was undertaken after the collect. This section describes the processing steps undertaken only for these data.

6.1 PREPROCESSING

All raw data acquired and stored in CD 1.1 format (CTBTO, 2002) on the nodes. The data are then extracted and converted to a *wfdisc* format (USNDC, 2010) used by our processing tools.

Our main post-processing tool is an internally developed and expanded tool suite termed *SeaTools*. *SeaTools* has the ability to read a number of different data formats, perform many signal and array processing applications (Smith, 2012; Smart and Flinn, 1971), and determine signal source locations (Lay and Wallace, 1995).

6.2 TARGET SELECTION FOR DETECTION

The processed data was selected using the firing times for these data (0Table 8). Each of the events was examined in *SeaTools* and processed. Many of the images in Section 0 not specifically from the SAIMA RDPS are from processing using *SeaTools*.

6.3 PARAMETER ESTIMATES

There are no parameter estimates for processing this collect.

6.4 CLASSIFIER AND TRAINING

No classifiers and training files were used for this analysis.

6.5 DATA PRODUCTS

The data products associated with this analysis are the raw and segmented data, and the processed images.

7.0 PERFORMANCE ASSESSMENT

For the purposes of reporting and describing the SAIMA system, several of the collects will be detailed, including one from APG and two from Ft. Sill. While only the last collect was funded during the ESTCP program, the other collects offer insight into the SAIMA system performance and validation. For convenience and readability, each of the results is described in separate subsections.

7.1 ABERDEEN PROVING GROUND (APG), MARYLAND

This collect and system test occurred on 28-29 November 2012. Five (5) nodes were deployed with radios to test the detection, location, and reporting of the system for 60 mm and 81 mm inert mortar impacts. The location and geological background were discussed in a prior section.

The array site locations are scattered around the field at approximately equal azimuths (Figure 11). This would be the most ideal position of a deployment around an impact field.

Figure 11. APG Impact Field with the Array Sites Dispersed Around the Field.

Nine calibration shots using 2.5 lb C-4 charge were positioned in the center of the field. Only four of these were recorded due to hardware issues (Figure 12). The four recorded locations were independently located within 2-3 m of the actual location whose coverage ellipses had a major axis on the order of 0.42 m.

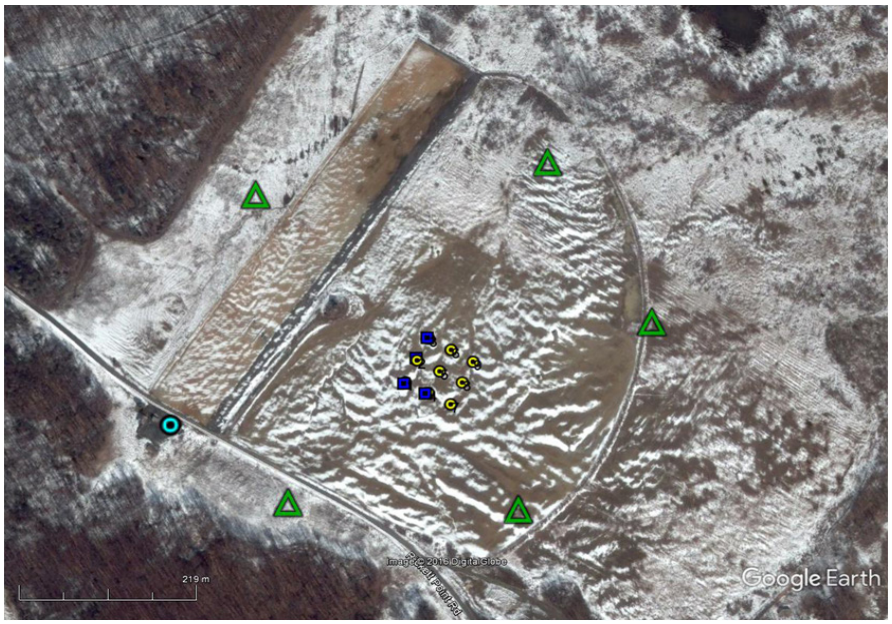

Figure 12. APG Impact Field with the Calibration Shots (Yellow Circles) and Located Positions (Blue Squares).

Following the calibration shots, mortar shots were fired into the field over a two day period. Both 60 mm and 81 mm mortars fired inert rounds into the field; some containing spotter charges (a small exploding attachment to the round). The mortars were fired from the west corner of the field at the position marked as FP (Figure 11). Most of the rounds were fired as Charge 1 to gain sufficient height for the shell path, resulting in higher kinetic energy impacts. Results obtained after detecting and locating offered good results; seven (7) are shown in this image (Figure 13).

Figure 13. APG Impact Field Seven (7) of the 81 mm Mortar Impacts with Spotter Rounds.

The next few figures illustrate the process. Figure 14 is a post-analysis image showing a typical unfiltered and filtered waveform data. The acoustic energy from the mortar tube is clearly visible. The impact of the 81 mm inert round is also clearly visible in the unfiltered data, not the filtered. A 100 to 300 Hz filter highlights the acoustic data from the shot at this scale.

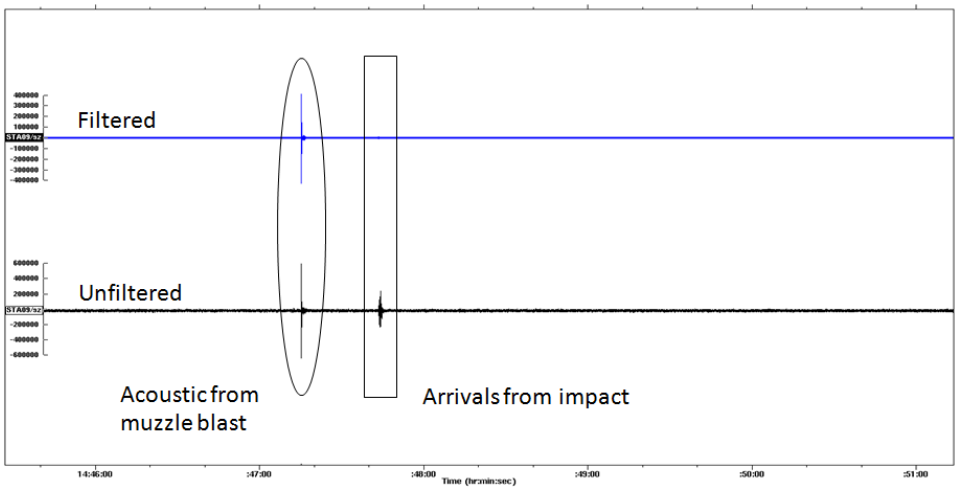

Figure 14. Filtered (100 to 300 Hz) and Unfiltered Data from an 81 mm Inert Shot on 29 November 2012 at 14:47 UTC.

The muzzle shot is clearly visible on both.

Zooming on the impact data (Figure 15), the unfiltered data has a beautiful seismic signal with a P-wave, probably an S-wave (or higher mode surface waves), and an Rg phase (bottom trace). So, the question is, what should be detected? Filtering the data between 100 to 300 Hz enhances the first arrival, cleans up the multiple phase arrives, and provides a clean signal for the detector (top trace).

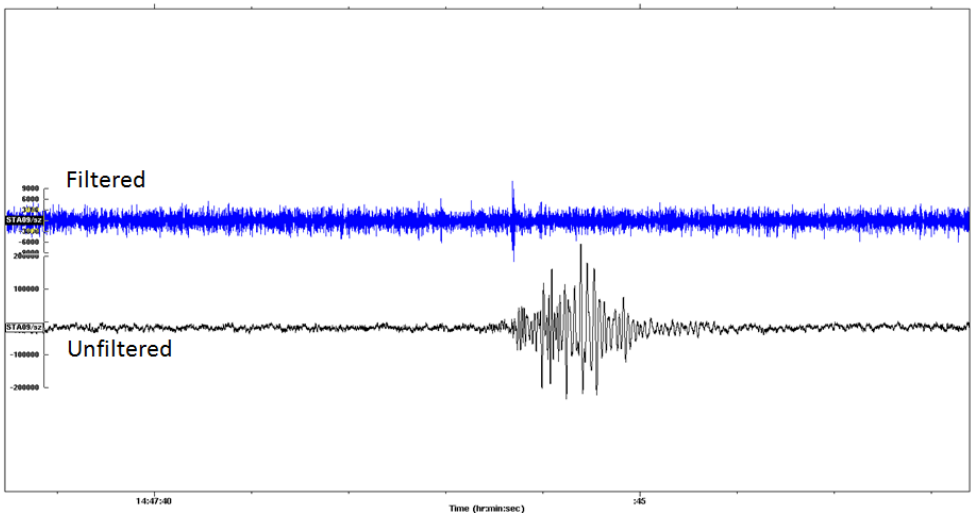

Figure 15. Filtered (100 to 300 Hz) and Unfiltered Data from an 81 mm Inert Shot on 29 November 2012 at 14:47 UTC.

The unfiltered arrival clearly shows what is probably a P-wave, an S-wave may be visible, and an Rg phase. Filtering the data enhances the first arrival of the P-wave.

Finally, zooming on the signal (Figure 16) provides a little more detail. Clearly, the filtered signal arrival corresponds to the P-wave onset and provides a good signal for the detector.

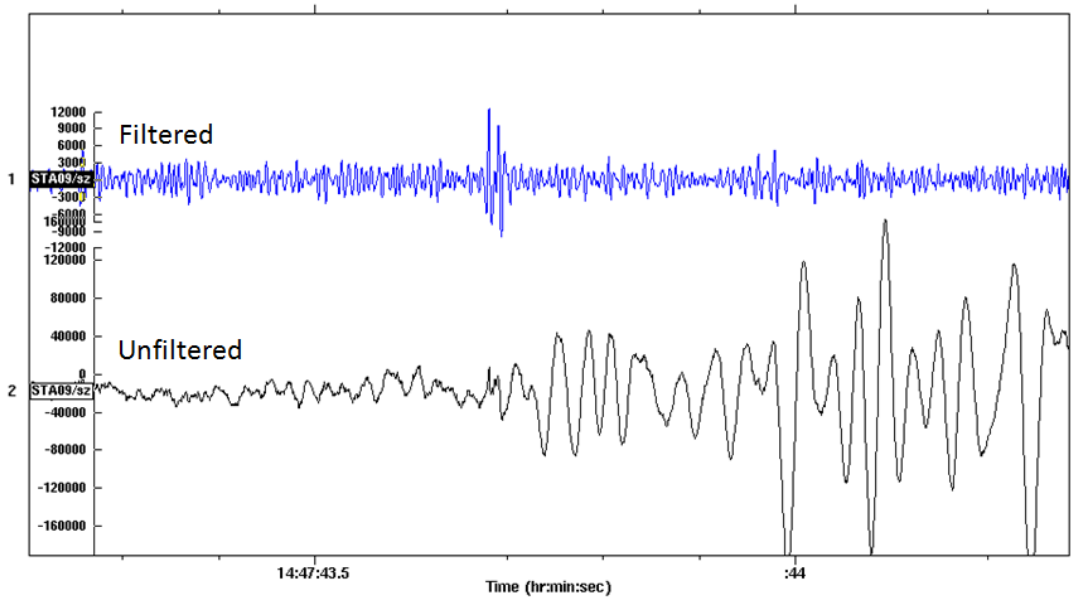

Figure 16. Filtered (100 to 300 Hz) and Unfiltered Data from an 81 mm Inert Shot on 29 November 2012 at 14:47 UTC.

This a zoomed portion of the prior image. Filtering the data enhances the first arrival (P-wave).

An example of the FK results from a spotter round is shown next (Figure 17). Note the clean signal from filtering that aids the phase pick allowing the FK to provide a tight results.

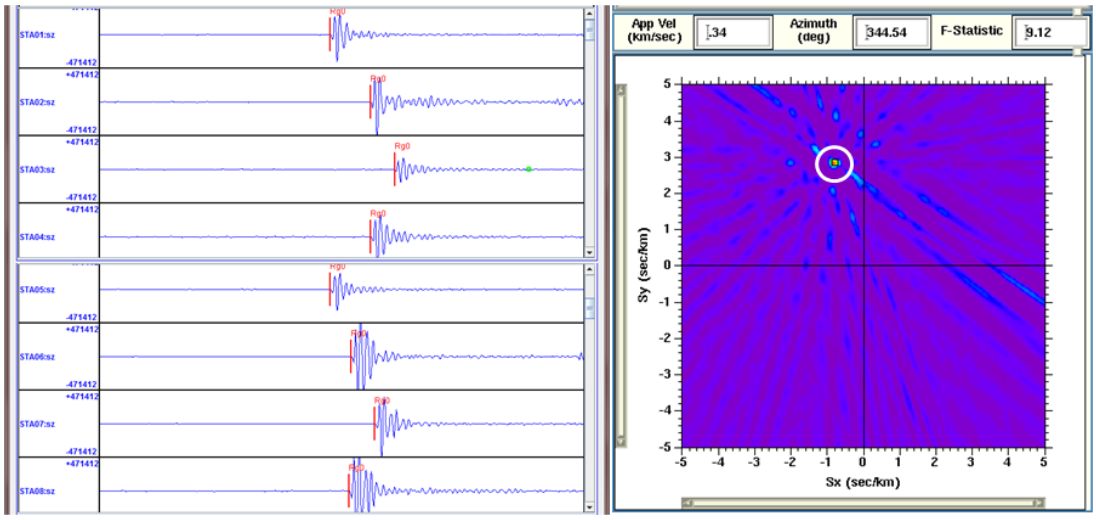

Figure 17. Filtered (100 to 300 Hz) 81 mm Spotter Round Showing the Automatic Detector Picks (Left Trace), Then Passed to the FK Algorithm to Determine the Azimuth and Slowness (Right Image).

Note the clear, tight coherent power of the FK (white circle).

Finally, the results of all stations are combined into the location algorithm to provide a location for the event, as shown by the yellow asterisk (Figure 18). Due to inhomogeneities in the ground, some azimuths may be slightly off. This is similar to wind pushing an acoustic wave. The location algorithm uses all information to provide a solution.

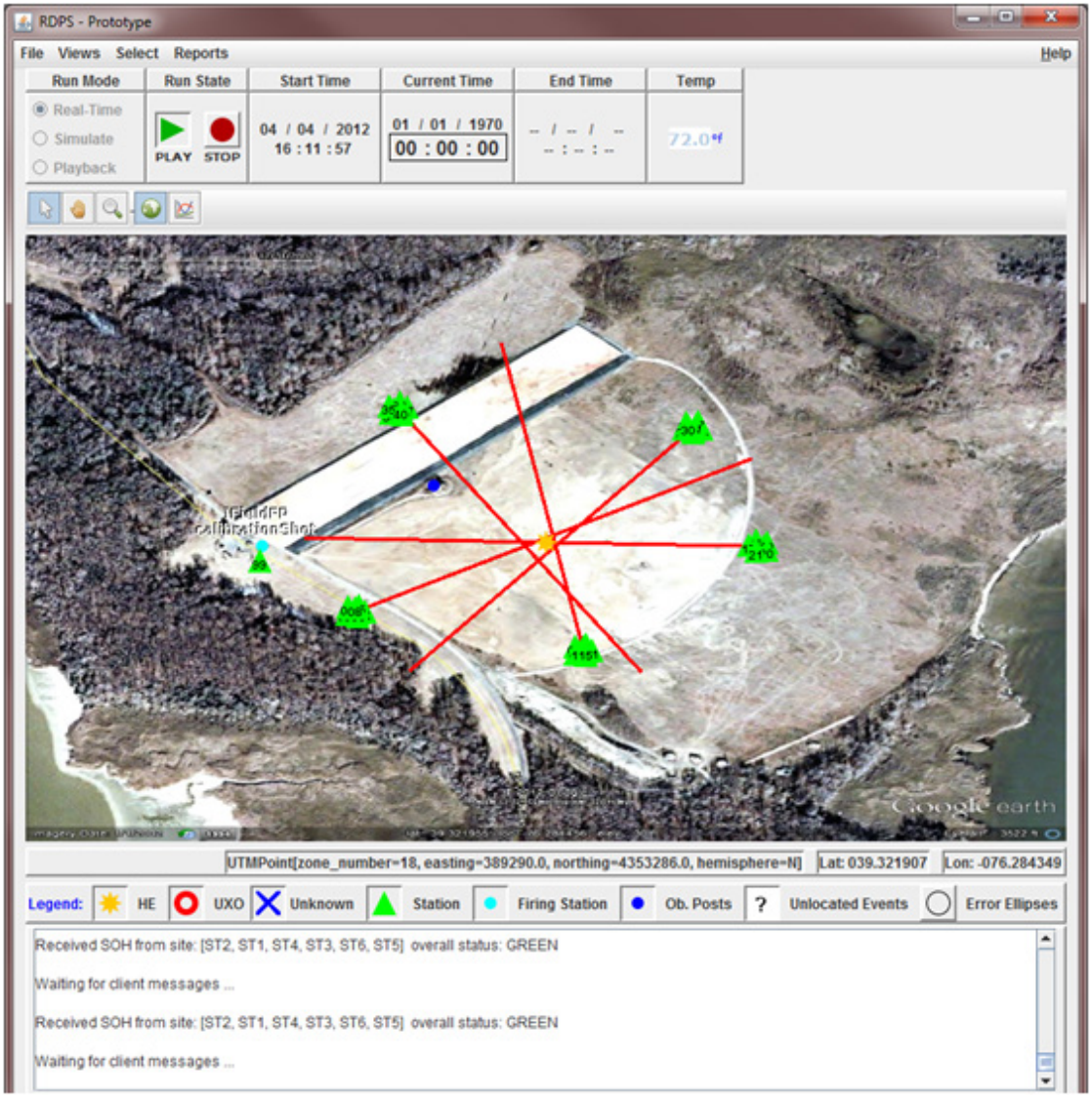

Figure 18. A Screen Capture of the Location Algorithm Results.

The individual beams are the azimuth results of the FK process at each site. At this site, the location combines the azimuths with the time, and locates the event (yellow star).

The location results from this experiment are shown in Table 2 through Table 5. The tables are split based on the different categories of shot. The "green" rows in Table 3 and Table 4 reflect rows where no node GPS information is available.

The location results were promising at this stage. Table 2 had a bad row with event #39; without this event, the mis-location error, the distance between the actual location and calculated error, was only 1.75 m. For the 81 mm inert rounds (Table 3), the mis-location error was only 4.82 m. With the 61 mm spotter rounds (Table 5), the mis-location error was only 1.3 m. This was a small field, but the impacts were also small, especially in the plowed ground of the impact field.

This effort was the first time an active field test of the equipment occurred, with radios, and against "live" targets. There were software bugs discovered during the deployment, but the collect helped to find and fix them. The results were very promising. The relevance of this collect and field trial should be kept in mind during the evaluation for this program.

Table 2. APG, 81 mm Spotter Rounds.

Round	Calib	Type	Date	Local time	GMT	Δ GPS (m)	sdobs	smajax (km)	sminax (km)	strike
16	81	Spotter	29-Nov-12	09:28:15	14:28:15	0.94	0.004037	0.001967	0.001892	150.80
17	81	Spotter	29-Nov-12	09:39:09	14:39:09	2.05	0.004242	0.001849	0.001761	155.26
22	81	Spotter	29-Nov-12	10:36:08	15:36:08					
27	81	Spotter	29-Nov-12	11:27:14	16:27:14	1.94	0.003825	0.001836	0.001772	150.35
32	81	Spotter	29-Nov-12	12:49:28	17:49:28	2.41	0.005366	0.002020	0.001953	153.35
37	81	Spotter	29-Nov-12	13:30:43	18:30:43	1.41	0.004019	0.001979	0.001920	146.55
39	81	Spotter	29-Nov-12	13:53:04	18:53:04	18.58	0.003728	0.002007	0.001946	145.93

Table 3. APG, 81 mm Inert Rounds.

Round	Calib	Type	Date	Local time	GMT	Δ GPS (m)	sdobs	smajax (km)	sminax (km)	strike
18	81	Dummy	29-Nov-12	09:47:14	14:47:14	73.10	0.005629	0.004745	0.003395	140.69
19	81	Dummy	29-Nov-12	10:01:53	15:01:53	5.92	0.008855	0.005191	0.003828	143.81
20	81	Dummy	29-Nov-12	10:11:58	15:11:58	4.82	0.006798	0.004553	0.003327	139.92
21	81	Dummy	29-Nov-12	10:19:42	15:19:42	-				
23	81	Dummy	29-Nov-12	10:46:26	15:46:26	7.18	0.008678	0.010713	0.004965	169.44
24	81	Dummy	29-Nov-12	11:03:57	16:03:57	4.14	0.034858	0.007505	0.006777	38.08
25	81	Dummy	29-Nov-12	11:13:12	16:13:12	58.91	0.002528	0.006148	0.003538	142.91
26	81	Dummy	29-Nov-12	11:20:20	16:20:20	42.43	0.001617	0.011085	0.005182	164.74
28	81	Dummy	29-Nov-12	11:33:56	16:33:56	54.51	0.008399	0.004180	0.003227	145.88
29	81	Dummy	29-Nov-12	11:42:01	16:42:01	42.09	0.003739	0.009348	0.005400	126.65
30	81	Dummy	29-Nov-12	11:52:28	16:52:28	1.38	0.004804	0.006067	0.003301	140.75
31	81	Dummy	29-Nov-12	11:59:37	16:59:37	4.85	0.004559	0.004429	0.002940	132.24
33	81	Dummy	29-Nov-12	12:57:18	17:57:18	-				
34	81	Dummy	29-Nov-12	13:06:41	18:06:41	53.79	0.004913	0.004456	0.003428	126.59
35	81	Dummy	29-Nov-12	13:14:41	18:14:41	7.68	0.004700	0.005815	0.003871	137.02
36	81	Dummy	29-Nov-12	13:20:59	18:20:59	50.52	0.002647	0.008380	0.004603	123.97
38	81	Dummy	29-Nov-12	13:38:21	18:38:21	67.52	0.011618	0.005820	0.004811	117.77
40	81	Dummy	29-Nov-12	13:59:37	18:59:37	2.64	0.023625	0.008203	0.006304	126.60
41	81	Dummy	29-Nov-12	14:06:17	19:06:17	58.02	0.014399	0.010984	0.005961	131.20
42	81	Dummy	29-Nov-12	14:13:12	19:13:12	842.73	0.002611	5.898545	0.014649	89.99

Table 4. APG, 60 mm Charge-1 Inert Rounds.

Round	Calib	Type	Date	Local time	GMT	Δ GPS (m)	sdobs	smajax (km)	sminax (km)	strike
7	81	Dummy	28-Nov-12	14:07:19	19:07:19	418.60	0.035495	0.211919	0.036422	160.09
8	81	Dummy	28-Nov-12	14:19:26	19:19:26	-				
9	81	Dummy	28-Nov-12	14:32:12	19:32:12	1.04	0.019887	0.009569	0.005008	134.42
10	81	Dummy	28-Nov-12	14:43:12	19:43:12	74.70	0.015612	0.012634	0.006467	132.82
12	81	Dummy	28-Nov-12	14:59:02	19:59:02	53.74	0.00582	0.012895	0.005903	148.59
13	81	Dummy	28-Nov-12	15:27:53	20:27:53	3.00	0.01218	0.009759	0.0048	129.87
14	81	Dummy	28-Nov-12	15:39:44	20:39:44	57.27	0.002321	0.007054	0.003576	136.2
15	81	Dummy	28-Nov-12	15:48:05	20:48:05	7.30	0.0269	0.008887	0.006483	133.46
44	60	Dummy	29-Nov-12	14:48:56	19:48:56	1022.00	0.031563	47.213530	0.182027	86.97
45	60	Dummy	29-Nov-12	14:58:19	19:58:19	1068.00	0.043239	70.347872	0.247473	86.96
46	60	Dummy	29-Nov-12	15:06:31	20:06:31	79.89	0.011339	0.008729	0.004585	130.09
47	60	Dummy	29-Nov-12	15:15:29	20:15:29	973.00	0.017600	10.541762	0.045373	87.07
48	60	Dummy	29-Nov-12	15:23:18	20:23:18	70.40	0.058429	0.105963	0.062819	122.92
49	60	Dummy	29-Nov-12	15:31:07	20:31:07	883,12	0.017819	12.194847	0.052950	87.46
50	60	Dummy	29-Nov-12	15:40:47	20:40:47	1060.70	0.008279	9.046877	0.030045	85.02
51	60	Dummy	29-Nov-12	15:49:25	20:49:25	3.69	0.006289	0.010722	0.005618	115.26

Table 5. APG, 60 mm Charge-1 Spotter Rounds.

Round	Calib	Type	Date	Local time	GMT	Δ GPS (m)	sdobs	smajax (km)	sminax (km)	strike
6	60	Spotter	28-Nov-12	13:58:16	18:58:16	0.67	0.002557	0.002725	0.002329	89.009
11	60	Spotter	28-Nov-12	14:51:17	19:51:17	0.83	0.003564	0.002158	0.002097	143.89
43	60	Spotter	29-Nov-12	14:41:14	19:41:14	2.37	0.003433	0.002054	0.002030	126.12

7.2 NORTH ARBUCKLE RANGE, FT. SILL, LAWTON, OK - EARLY WORK

There are several field collects detailed in this section The first was a collect and system test that occurred in 2012, from 22 June to 1 July. Three (3) nodes were deployed with radios to test the system performance in the detection, location, and reporting of the system for 105 mm and 155 mm HE impacts using a larger impact field. A prior section discussed the location and geological background.

The site locations were scattered around the southern part field at approximately equal azimuths (Figure 19). This is a sparse network for a field this size.

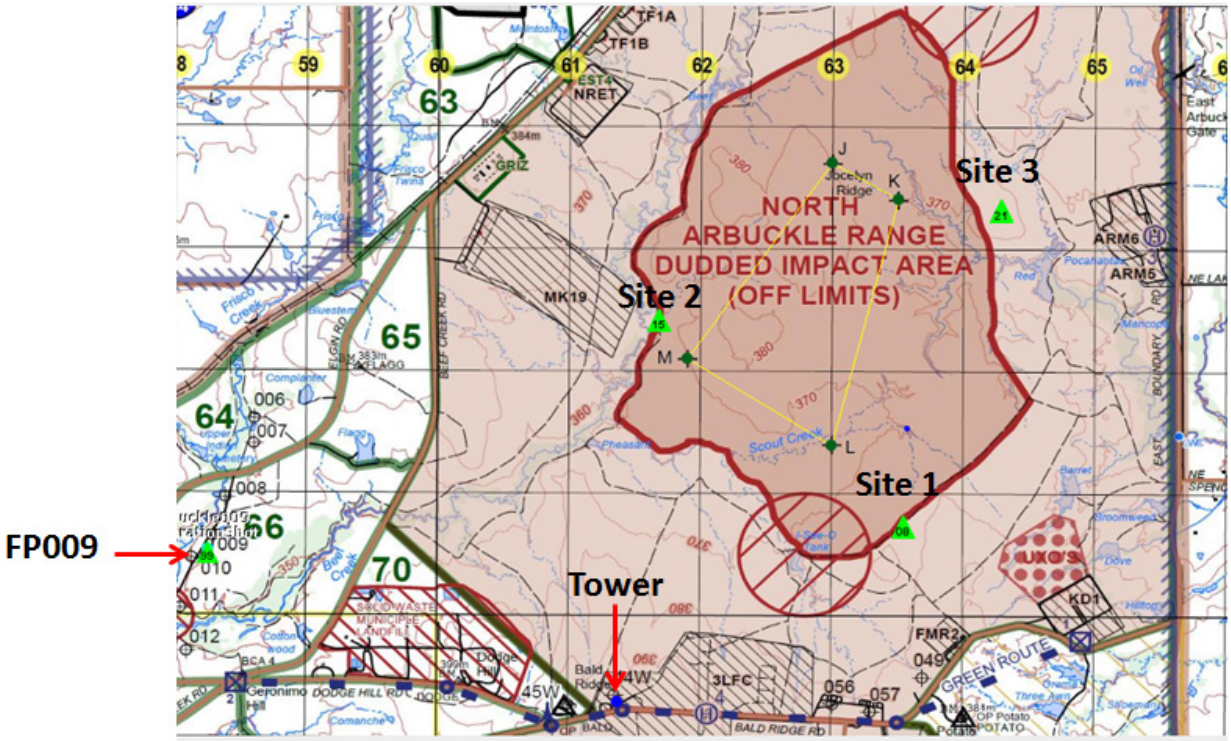

Figure 19. The North Arbuckle Range with the Dudded Impact Area and the Three Array Sites Along the Impact Area Firebreak.

The tower containing the RDPS along the southern border and firing point (FP009) positions are also shown.

Over a three day period, over 400 rounds of both 105 mm and 155 mm were fired into the field (Table 6). Issues with the nodes resulted in some data loss (the Missed column), but all others were located by the system performing in a routine manner. In other words, the trigger node sent the signal downrange via the RDPS, each node captured and processed the proper signal, then sent the information back to the RDPS for location processing and capture. The remaining or captured events, 187 events or 46%, were located.

Table 6. Ft. Sill, June 2012, Rounds Fired and Located.

Date	Total Shots	Types	Located	Missed
26 June 2012	134	*78 105 mm* *56 155 mm*	45	89
27 June 2012	132	*76 105 mm* *56 155 mm*	124	8
28 June 2012	137	*74 105 mm* *63 155 mm*	18	119

The daily locations are shown in Figure 20 through Figure 22. Many of the locations were only obtained with 2 of the array stations due to random node outages.

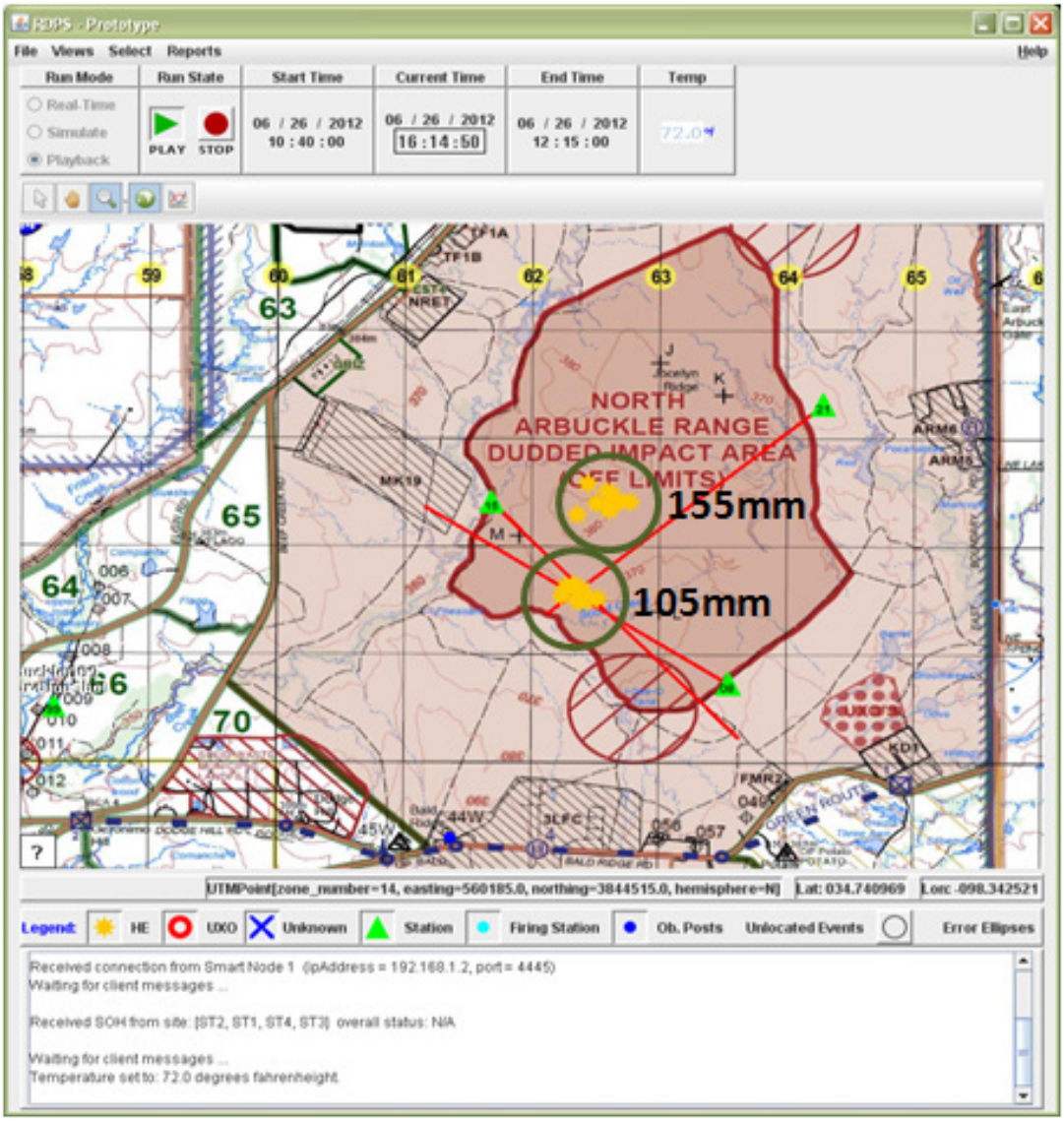

Figure 20. Screen Capture of the RDPS for 26 June with the Split 105 mm and 155 mm Impact Locations Marked.

All yellow asterisks were located by the SAIMA.

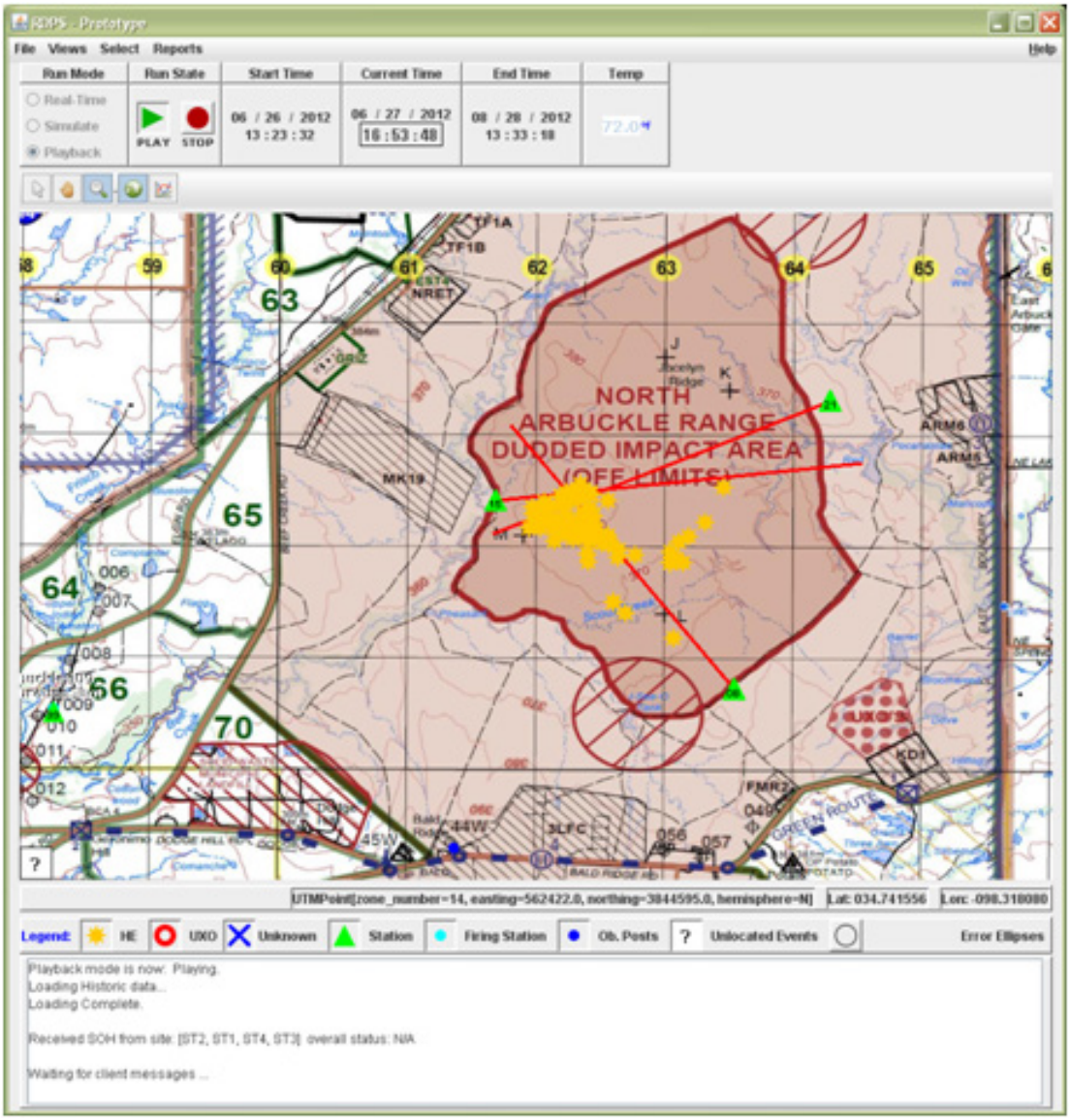

Figure 21. Screen Capture of the RDPS for 27 June.

All impacts were in one location except a few outliers. All yellow asterisks were located by the SAIMA.

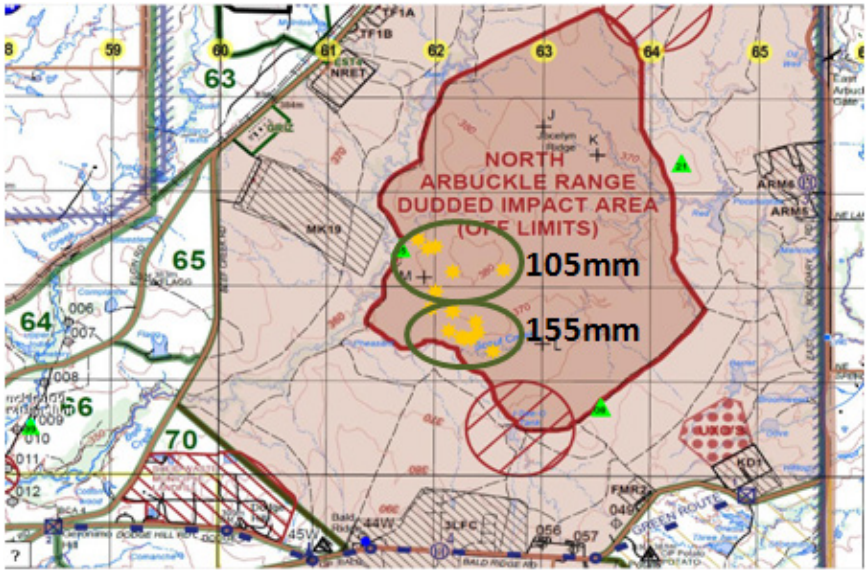

Figure 22. Screen Capture of the RDPS for 28 June with the Split 105 mm and 155 mm Impact Locations Marked.

All yellow asterisks were located by the SAIMA.

The main issue with this collect was the reliability of ground truth on the impacts. Cameras were used to get optical bearings on a few events. Figure 23 illustrates the "ground truth" and SAIMA location differences using different symbols. These are only 20 155 mm events located using all three array sites. Coverage ellipses are on the order of 5 m by 10 m. However, cameras and an inadequately detected calibration shot suggest the location bias (mis-location) may be between 20 m to 200 m, a much larger value. It is not possible to GPS the impacts at this location.

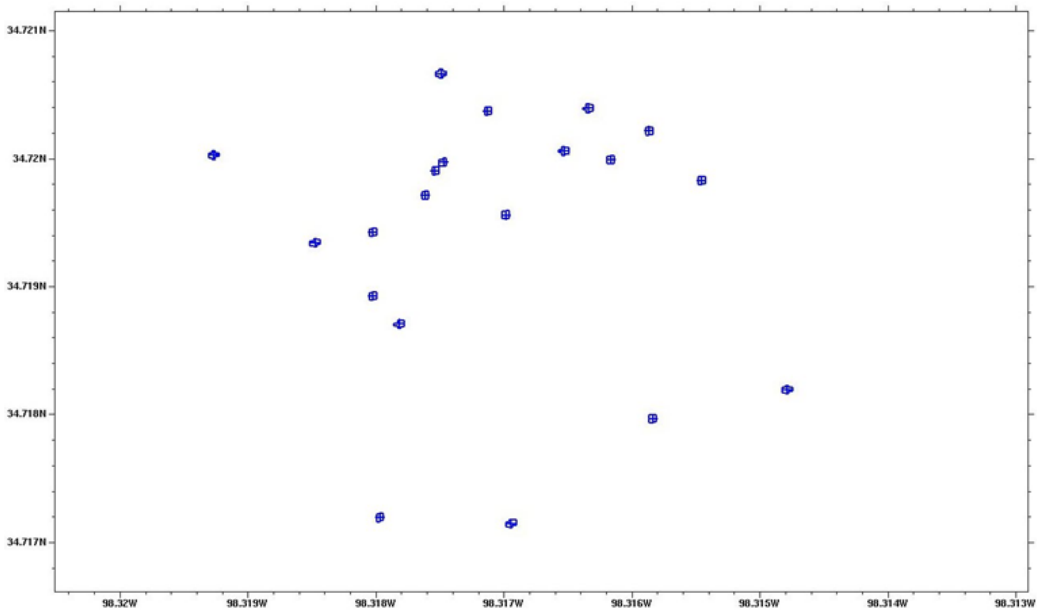

Figure 23. Acoustic Locations and Located Events for the 20 155 mm HE Events Observed by All Three Array Sites.

It should be clear that SAIMA can be used to detect and locate large SNR events, i.e. HE. The Ft. Sill range is on the order of 3 km by 3 km in the southern half. Coverage ellipses of 10 m on the 3000 m by 3000 m range are good but could be smaller with better coverage. However, the location bias must be known to better locate the impacts. The location bias can be determined by either using calibration shots (or blasts), or having known locations for several rounds using GPS.

Finally, three arrays were shown to be inadequate for a field this size. In August 2013, five (5) arrays were installed along the southern perimeter of the North Arbuckle Range at Ft. Sill, essentially adding two arrays. The arrays were positioned to provide the maximum azimuthal spread in the lower field and positioned to take advantage of the impact zones observed in prior trips to Ft. Sill (Figure 24).

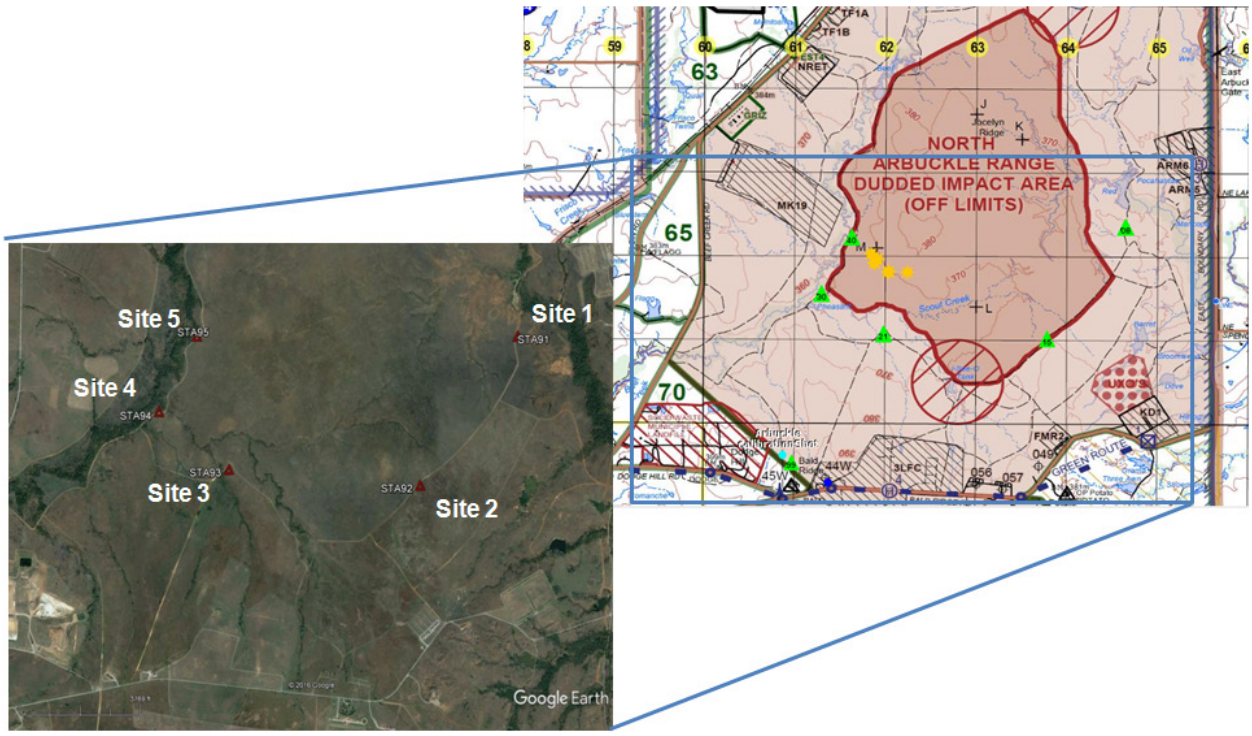

Figure 24. Location of the Five Array Sites at Ft. Sill, Installed August 2013.

Each of the sites was equipped with eight (8) sensors using the same array pattern (Figure 8), a solar panel with two (2) batteries, a node, and radio mast for the 900 MHz antennae (Figure 25). The sites were installed, briefly tested with one day of firing, and left with range control to evaluate.

Figure 25. A View of the Node and Battery Assembly with the Solar Panel (Top), and an Installed at Ft. Sill (Bottom).

7.3 NORTH ARBUCKLE RANGE, FT. SILL, LAWTON, OK - ESTCP

The most recent work at Ft. Sill began in June 2014. This effort had the objectives of collecting UXO (from duds fired into the range), low and high order detonations, and fire for effect. The main goal was to demonstrate P-wave could be detected and used to locate the UXO impacts, achieving some small coverage ellipse to bound the impacts.

In August 2014, a trip was undertaken to Ft. Sill to evaluate the system left in the field August 2013. It was determined that several of the prototype systems had failed, but it was thought several could be reactivated to perform the collects needed for the ESTCP Phase I effort. If necessary, additional equipment could be supplemented to fill any coverage gaps.

However, the inert munitions took much longer to collect, transfer to the range, and arrange to fire than thought possible. Not until 13 October 2016 did everything get organized to fire the inert munitions; this was after a couple of false starts during the summer of 2016. [NOTE: as a result of deploying for one trip, but discovering conditions were not acceptable, additional funding was added to the contract.]

However, by this time, none of the equipment from 2013 was deemed useable. To compensate, QTSI temporarily fielded two arrays inside of the western edge of the impact zone with several single channel units to help guide the analysis (Figure 26). Firing constraints and field access limited equipment installation.

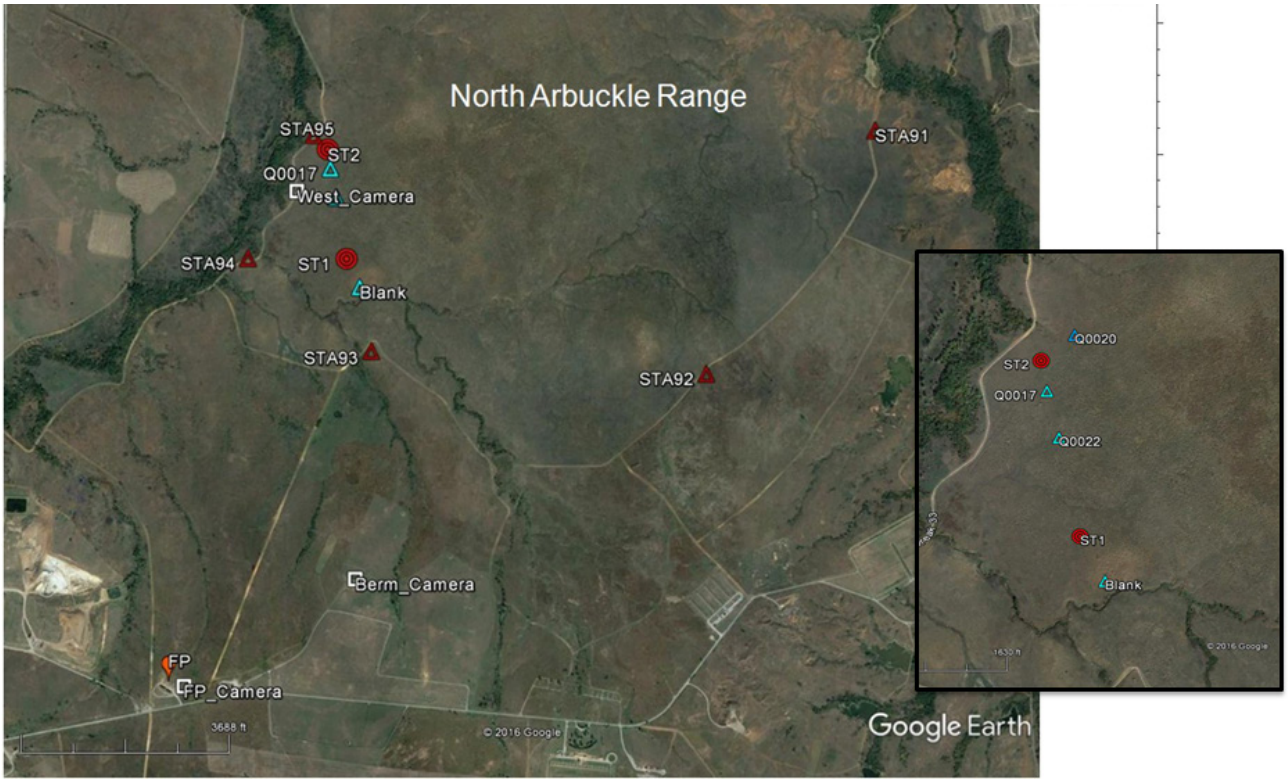

Figure 26. View of the Temporary Station Locations in October 2017, the Firing Point (FP), and Camera Locations (West-camera and Berm-camera).

Twenty-four inert munitions, 155 mm, were obtained to be fired during a normal training class firing 155 mm and 105 mm HE, a total of 142 total rounds (Appendix C, Table 8). Four guns were firing: a Paladin (155 mm), an M777 howitzer (155 mm), and two 105 howitzers (M119A2). These were established at the firing point marked FP (Figure 26). A view of the munitions (Figure 27) provides a scale of the bullets. The HE 155 mm are in yellow; the inert 155 mm munitions have the blue rings. No inert 105 mm munitions were available.

Figure 27. View of the Gun Placement at the Firing Point (FP) and Ammunition Pallets.

A typical HE waveform easily illustrates the type of signals observed when the munition explodes (Figure 28). Two HE events are shown from two arrays: one in black (only two elements are shown), the other in blue. Note the acoustic muzzle blast crosses each array at different times. When the munition explodes, the HE wave also crosses the two arrays at different times.

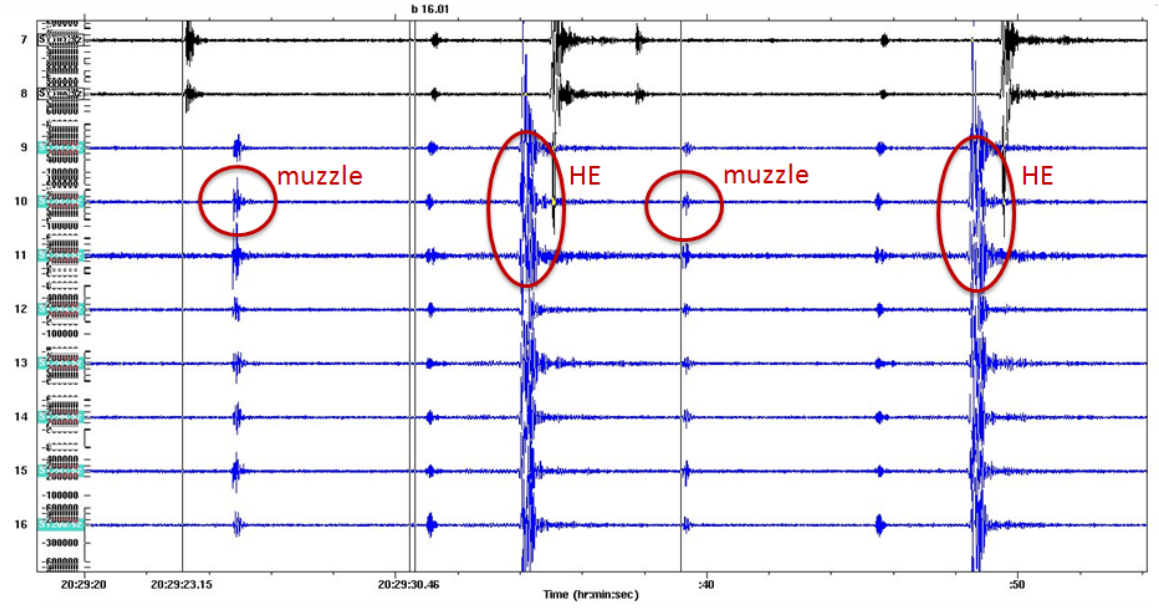

Figure 28. Waveform for the HE Events #44 and #45 (155 mm) on 13 October 2017 Beginning at 20:29 UTC.

The waveforms are filtered between 10 to 150 Hz.

Using an fk-trend (Figure 29) calculated on ST1, the random pattern of FK background shows a constant azimuth (top trace) when the muzzle acoustic wave crosses the array and when the HE acoustic crosses the array, although each are at different azimuths. An fk-trend is a result of performing multiple FK windows at equal time intervals along a waveform segment, then preserving the azimuth, apparent velocity, and F-statistic at each interval. Trends in coherent energy are more visible with this type of analysis. Note the muzzle azimuth points back towards the source, the HE acoustic toward the direction of the HE. Each are associated with a higher F-statistic value indicated a measure of coherence in the signal.

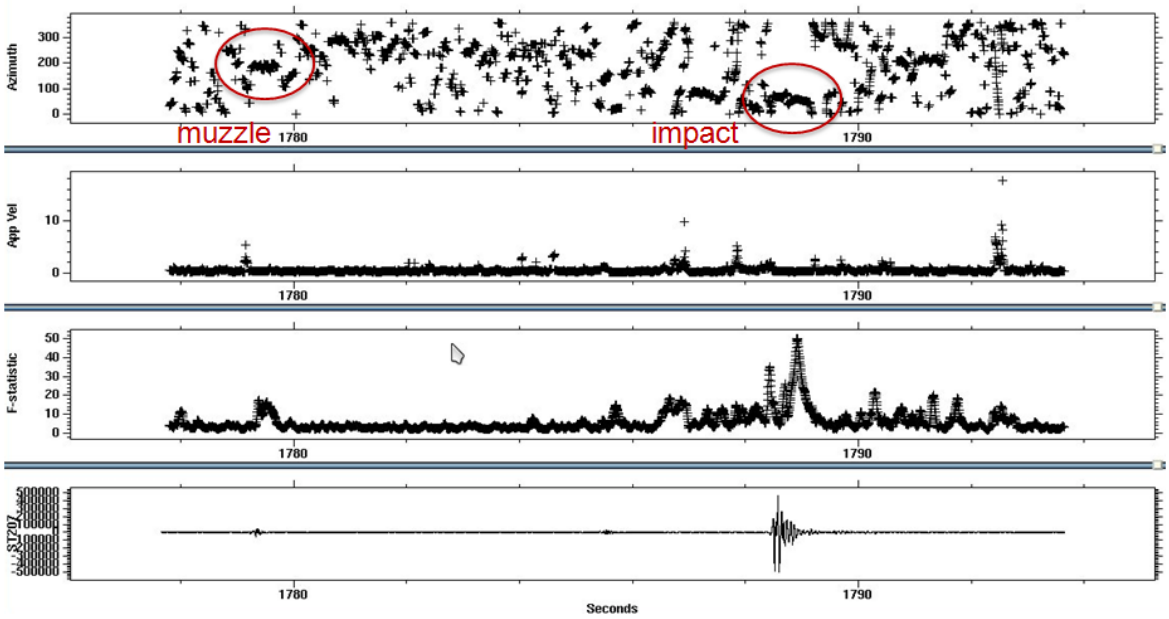

Figure 29. fk-trend for HE Event #44 (155 mm) on 13 October 2017 Beginning at 20:29 UTC on ST1.

The muzzle and explosion signals are circled.

The various HE events were plotted using just the acoustic azimuths from two sites. The results are shown for both the 155 mm and 105 mm HE (Figure 30). Note these were only located with the two array stations to the west of the impact area. with a cross-wind, east to west and the location bias from the two arrays on the west, all resultant locations will be pulled to the west by some amount. To determine the degree of offset, several events were optically located using two cameras set at orthogonal angles, west-camera and berm-camera (Figure 26). The results are shown by the three triangles (Figure 30). Due to the windy day with a light drizzle and fog near the ground, the impacts were difficult to determine from the cameras, thus the low number. All acoustic locations are offset to the west.

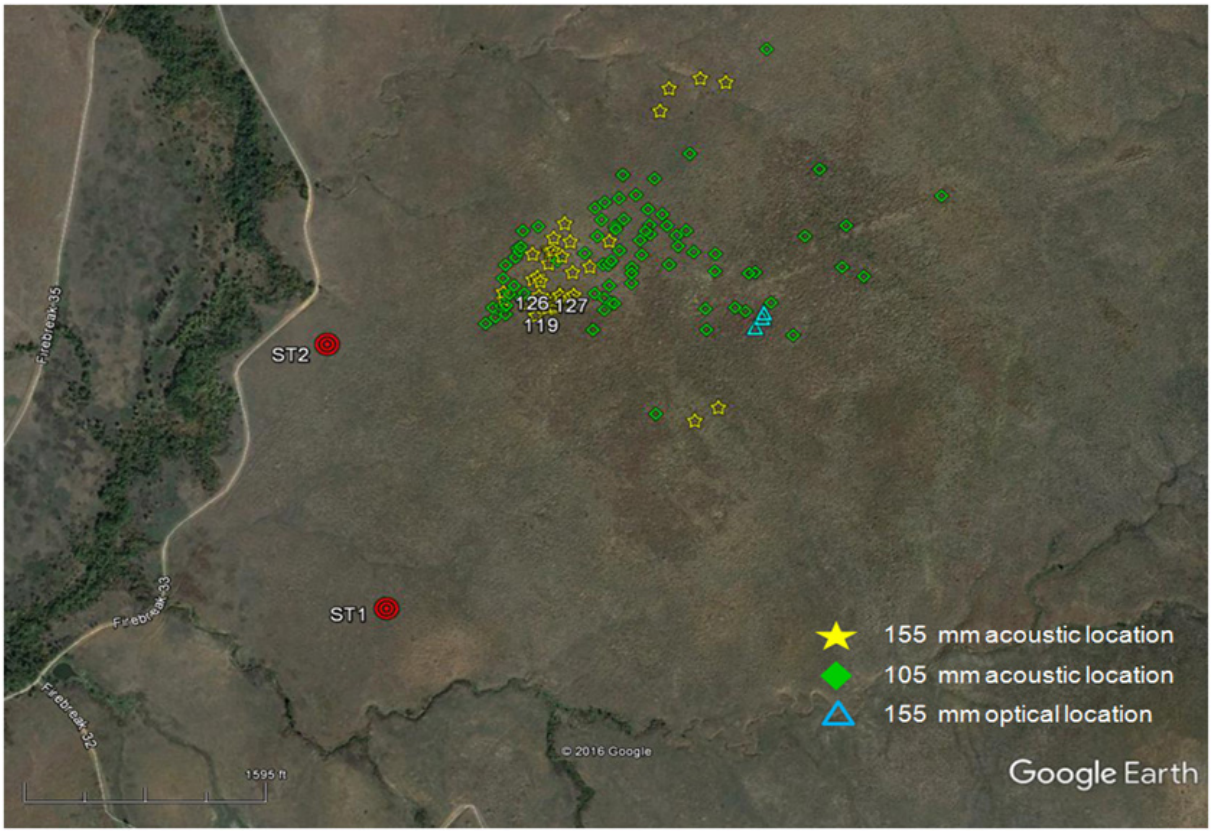

Figure 30. Azimuthally Located HE events for both the 105 mm and 155 mm howitzers.

The optically located events are shown by the triangles.

One of the main objectives for this effort is whether the system can determine the impacts from UXO. These were mimicked by the insert rounds. Waveforms from all inert events were examined. Figure 31 and Figure 33 show the waveforms from an event (#25 at 19:14 UTC) filtered between 10 and 100 Hz. The muzzle acoustic signature is clearly visible, and for these events, the kinetic impact of the signal is also clearly visible.

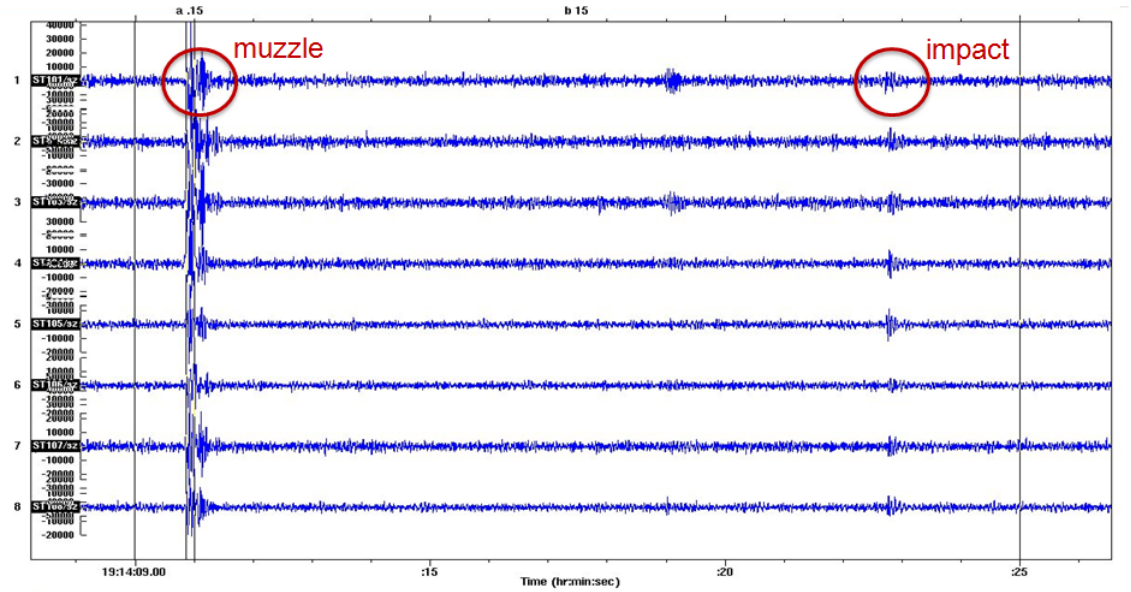

Figure 31. Waveform Recorded at Array ST1 for Inert Event #25 (155 mm) on 13 October 2017 Beginning at 19:14 UTC.

The waveforms are filtered between 10 to 100 Hz.

To assist with recognizing the inert impact signatures, the fk-trend analysis was performed on all inert events. Figure 32 and Figure 34 illustrate the results for this event at these two arrays. The inert impact signature at ST1 is clearly visible at an azimuth of approximately 20º while it is less clear but recognizable at ST2 at an azimuth of 77º. The acoustic muzzle signature at both arrays is clearly coherent.

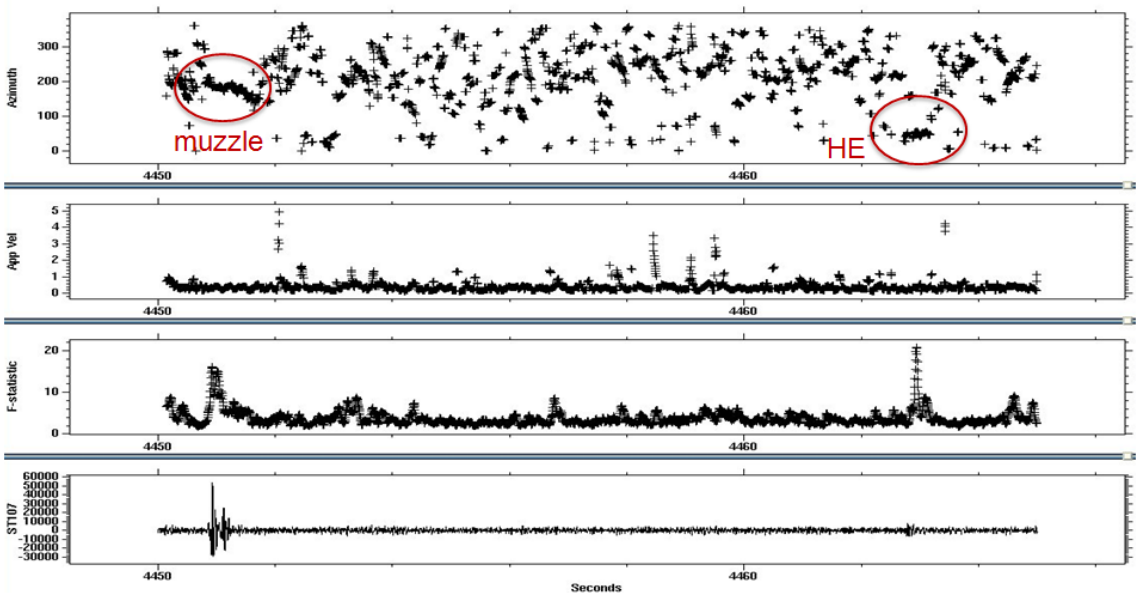

Figure 32. fk-trend of the Waveform Recorded at Array ST1 for Inert Event #25 on 13 October 2017 Beginning at 19:14 UTC.

The muzzle and explosion signals are circled.

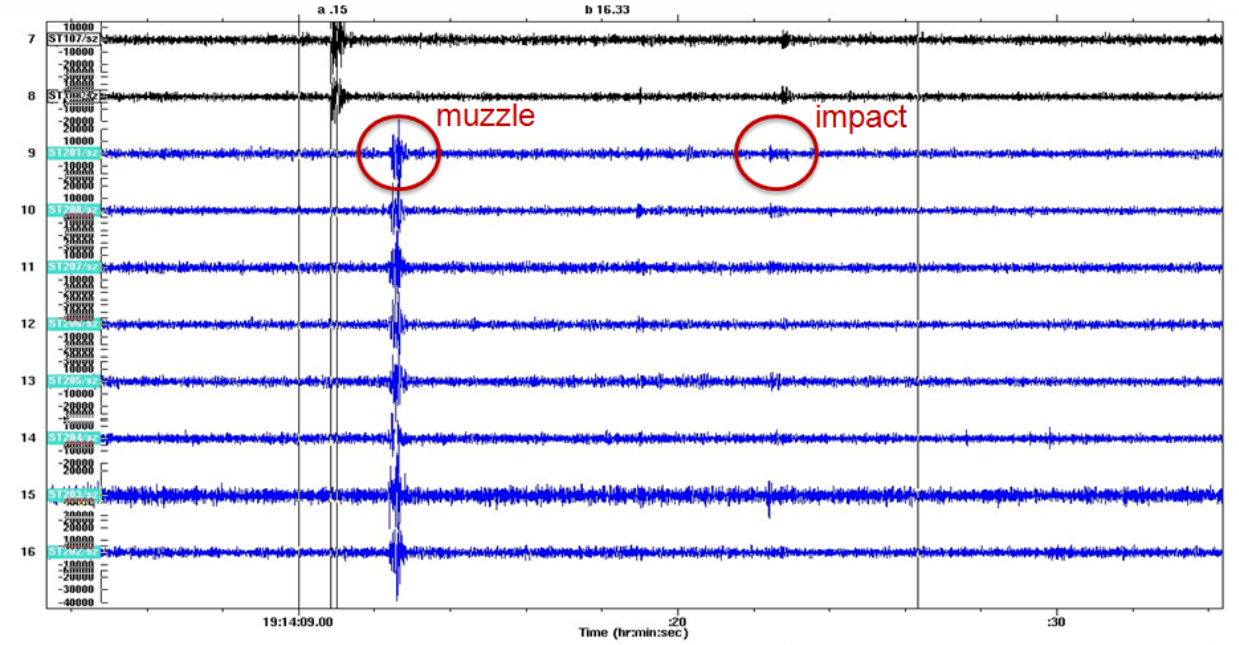

Figure 33. Waveform Recorded at Array ST2 for Inert Event #25 (155 mm) on 13 October 2017 Beginning at 19:14 UTC.

The waveforms are filtered between 10 to 100 Hz.

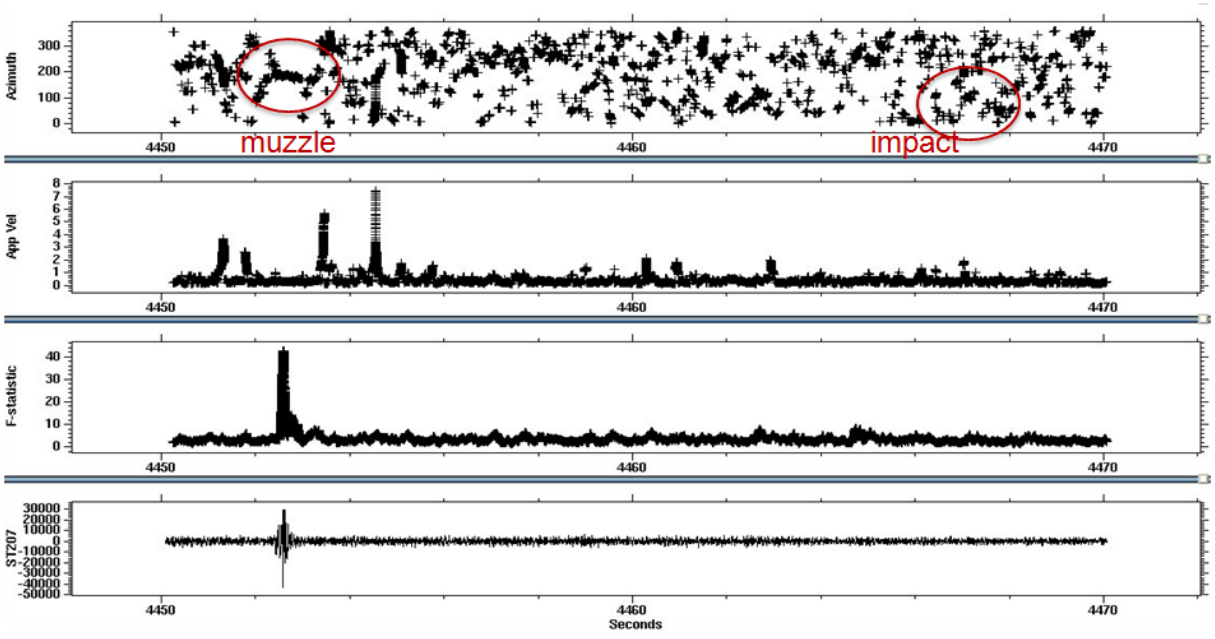

Figure 34. fk-trend of the Waveform Recorded at Array ST2 for Inert Event #25 on 13 October 2017 Beginning at 19:14 UTC.

The muzzle and explosion signals are circled.

This analysis was followed for all 23 inert rounds. The result, 10 of the 23 rounds were located (Figure 35). The inert rounds are located much closer to the optical locations from the cameras.

However, they appear to have much more scatter. A denser station network should allow all inerts to be located; the inerts were reliable located at distances of 800 m.

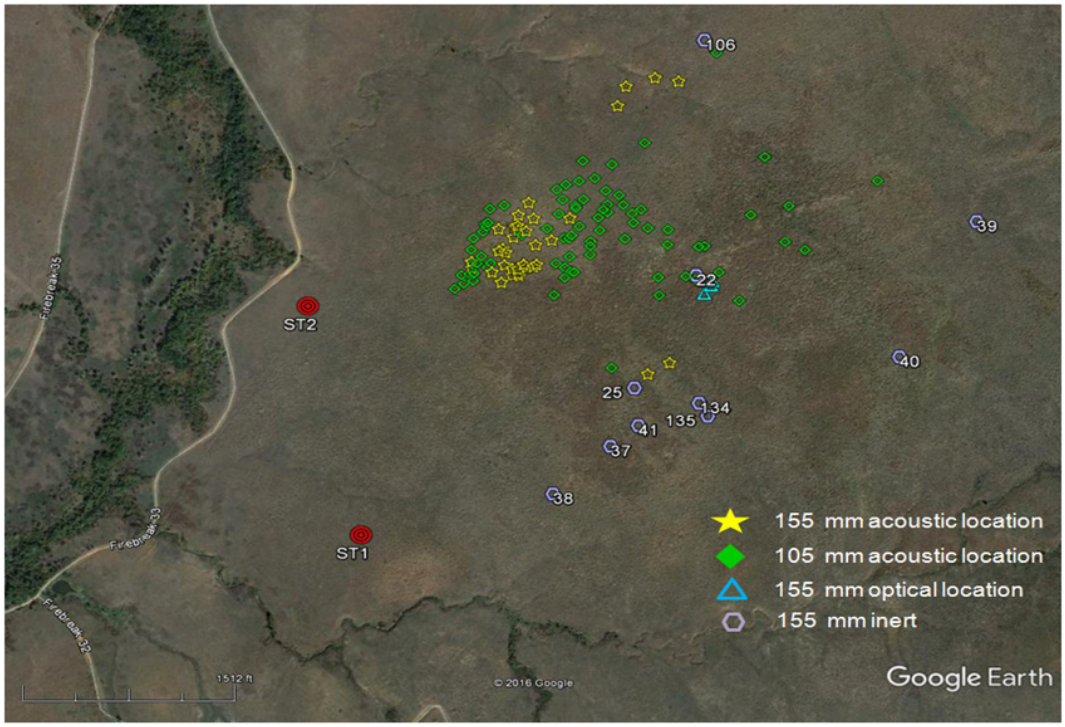

Figure 35. Seismically Located Inert Events Shown with the HE Event Locations.

Part of this scatter may be the result of the cadet training firing the guns. Recall in Figure 28 a small signal between the marked muzzle and HE phases on the waveforms is observed. Examining a small group of these from each array and from both the HE and inert rounds, note the variability of the delay as a result of different fire groups (i.e. different groups of cadets). The rounds are much similar for the HE group than for the inert rounds (Table 7).

Table 7. Delay Time Between the Acoustic and Extra Phase (Seconds) at Each Array.

Shot #	HE	
	ST1	ST2
30	6.15	4.49
31	6.18	4.53
44	7.91	6.27
45	7.87	6.21
52	8.46	6.60
90	8.07	6.44
91	7.97	6.38
93	8.09	6.45
118	6.31	4.71
119	6.25	4.65
126	6.08	4.43
127	6.14	4.48

Shot #	Inert	
	ST1	ST2
22	7.90	6.33
38	5.97	4.42
40	5.80	4.28
41	5.90	4.40
46	2.55	1.78
47	2.47	1.19
48	2.49	1.64
49	2.35	1.71
50	2.49	1.10
51	2.39	1.67
94	2.13	2.50
95	2.31	1.09
98	2.29	1.26
99	2.28	1.08

The origin of this small phase was explored. Event #46, at 20:37 UTC, at array ST2 provided the clue. Note the "choppy" or "spiky" nature of the waveform following the acoustic phase (Figure 36). The fk-trend from this resulted in a coherent signal changing in azimuth (Figure 37). The key is this coherent signal changing in azimuth as a function of time (circled). Converting the seismic files to a purely acoustic file, then listening to it, shows this is the shell passing overhead tumbling; a distinct "wop-wop-wop" can be heard; the shell is tumbling The same analysis on an HE, for example Figure 29, has a cleaner path through the air, and only a small "whoosh" as the shell passes over the array.

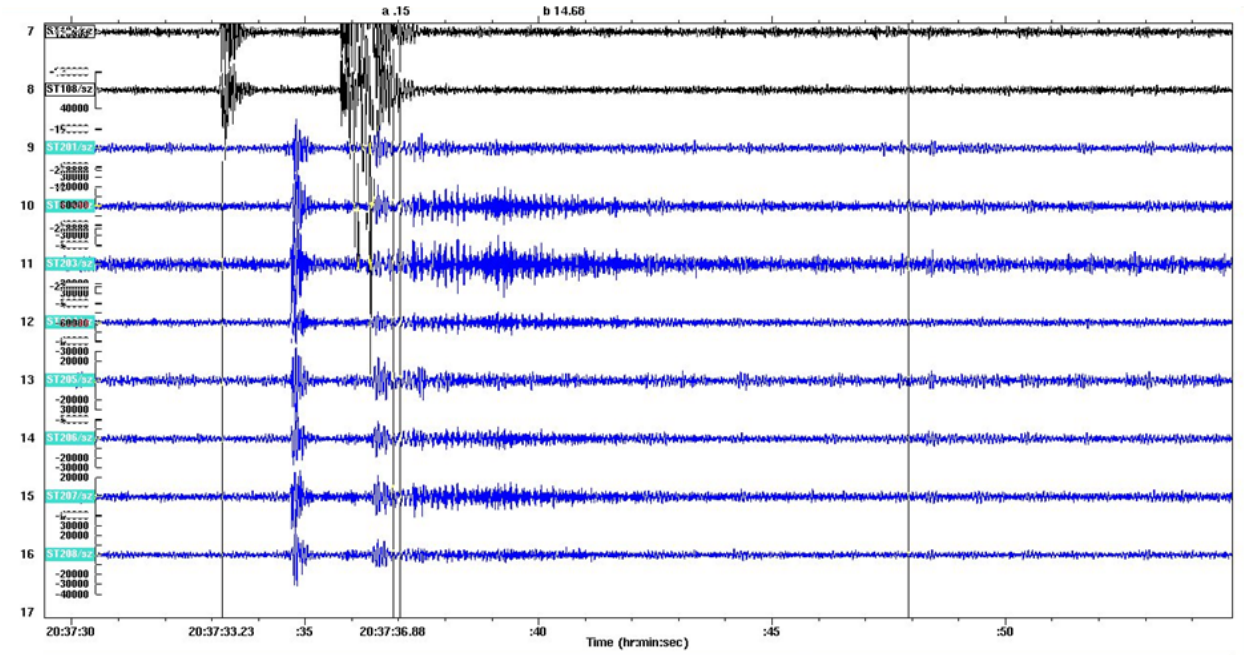

Figure 36. Waveform Recorded at Array ST2 for Inert Event #46 (155 mm) on 13 October 2017, 20:37 UTC.

The waveforms are filtered between 10 to 150 Hz.

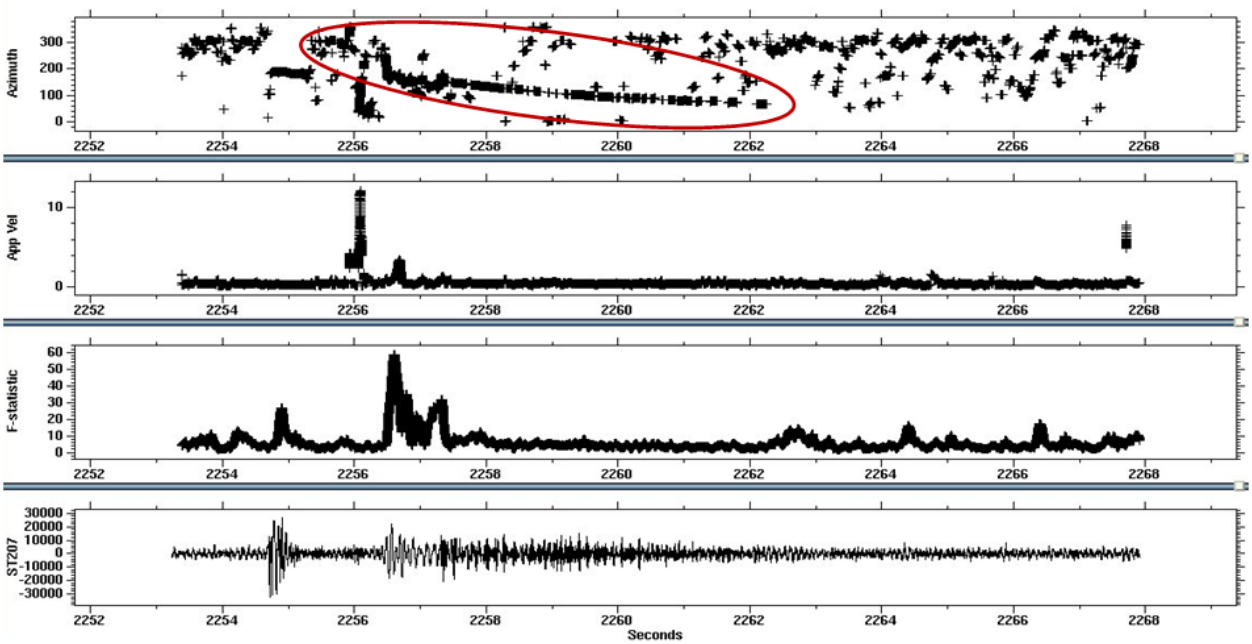

Figure 37. fk-trend of the Waveform Recorded at Array ST2 for Inert Event #46 on 13 October 2017, 20:37 UTC.

The circled segment is the path of the shell; the azimuth is changing as a function of time.

The result is a distinct possibility the inert rounds may be more unbalanced and may tumble more, resulting in greater scatter in their location. The scatter in the time delay between the acoustic and shell passing overhead (Table 7) further suggests the students, instructor, or both had to change the gun angle more for these rounds than for the HE rounds.

7.4 OVERALL PERFORMANCE ASSESSMENT

This section summarizes the performance against the objectives listed in Table 1. A quick summary of the objectives are:

- Assess quality of the SAIMA system currently deployed at Ft. Sill,
- Collect and analyze data for UXO detections, and
- Collect and analyze "fire for effect" for single dud detections

Additional details concerning performance are found earlier in this section (Section 0).

At the beginning of the effort, August 2014, a reconnaissance trip to Ft. Sill was undertaken to assess the equipment deployed in August 2013. At that time, an evaluation stated the equipment could be restored to working order. This would have allowed five (5) sites to sample the field when firing the inert rounds (0Ft. Sill, Equipment Assessment, August 2014.).

Due to the delays in acquiring the munitions (finding, funding, transfer to Ft. Sill, arranging a firing schedule), the equipment was not salvable. To overcome the problem in an attempt to acquire useable inert rounds, Quantum donated equipment to use during the collect in October 2016.

Firing schedules at Ft. Sill prevented insufficient range access time to install more equipment than was installed. Additional time would have allowed sites to the south and east of the impact area, reducing the propagation path distances and providing better azimuthal resolution.

With the issues just stated, two arrays were installed and recorded HE impacts and inert impacts. For the first time, seismic impacts were observed and utilized to recover impacts from inert rounds, mimicking UXO rounds. This was a major accomplishment for this effort.

The artillery officer was unable to provide a "fire-for-effect" scenario; these data could not be obtained. Without the data, this objective could not be met. Any future work should provide dedicated fire control on the range to obtain the needed data for assessment.

While not shown during the collect during October 2015, the SAIMA system has been shown to automatically trigger, process, and locate rounds, whether mortar or artillery, and report the location to the user. This last effort demonstrates UXO will be detected and located given a sufficient station density.

With the prior deployments and success of this last collect to actually detect and locate inert rounds, the SAIMA program has been shown to be a success. Overcoming the issues of sufficient range time to install equipment and to provide a dedicated fire mission to test and demonstrate the automated SAIMA system, should provide a success during the Phase II OPTION.

8.0 COST ASSESSMENT

This section contains the Cost Model, Cost Drivers, and Cost Benefit analysis.

8.1 COST MODEL

For this project, a seismic/acoustic system was used to collect UXO (duds) during a munitions training exercise at North Arbuckle Range, Ft. Sill, OK, and demonstrate SAIMA capability to detect and locate the impacts on range. This report addresses Phase 1 of the two-phased project that collected data to show specific aspects of this technology's performance before committing to a full-scale deployment and demonstration in Phase 2. The proposed work of the Phase 2 OPTION is to deploy, test, and demonstrate a full-scale test system around the entire North Arbuckle Range Dudded Impact Area which is approximately 8 km^2. Therefore, the best cost model to use in this Phase 1 Final Report is the proposed cost of Phase 2 of the current ESTCP contract. Once Phase 2 is completed, Quantum will then have sufficient data and information to provide a fact-based cost assessment in the Phase 2 Final Report. For reference, the total contracted cost for the Phase 2 OPTION (Tasks 3 through 7) is $620,720, where $544,229 of that is for Quantum's work and $76,491 is for Government support.

8.2 COST DRIVERS

By the nature of the technology, Quantum expects the principle cost drivers deploying and operating the SAIMA system are:

- Scale of the munitions to be detected and located; ground impact of smaller artillery/mortar UXO (dud) rounds (*e.g.*, 60 mm and 81 mm) will require more stations for a given impact area than will large artillery rounds (*e.g.*,105 mm and 155 mm)
- Size and shape of impact area; very large impact areas and those with oddly shaped boundaries will require more stations to monitor, and especially large impact areas may require stations located inside the impact area boundary.

8.3 COST BENEFIT

The cost benefits are derived principally from accrued savings over the long-term. Deploying operational SAIMA systems on future DoD live ordnance ranges will gradually reduce continuing contributions to the UXO/MC cleanup challenge by locating these rounds and allowing range managers to remove them routinely over the life of the impact area. Although this will take decades because of the need for cleanup efforts when ranges are closed and remediated, with the universal deployment of SAIMA systems that cost will steadily decrease and eventually be eliminated. Furthermore, with relatively modest adaptations, the SAIMA system could also provide DoD air-to-ground bombing ranges the same service.

9.0 IMPLEMENTATION ISSUES

During normal installations, the SAIMA system can be deployed quite easily. Projected times for installation (a rule of thumb) are approximately one day per site. This includes setting the trigger node, all sensors at each array site, RDPS site, and array and radio tests between all sites.

During this last collect, temporary stations (two arrays and four single channel units) were deployed powered by batteries with no radio signals. All equipment was deployed in one day with EOD support to access the field.

In this collect, time to access the range was the issue.

10.0 REFERENCES

Akaike, H. (1974). A new look at the statistical model identification, *IEEE Trans on Automatic Control*, **19**, 716-723.

CTBTO (2002). Formats and Protocols for Continuous Data CD-1.1, IDC Software Documentation, Preparatory Commission for the Comprehensive Nuclear Test Ban Treaty Organization, IDC 3.4.3, 18 December 2002.

Diehl, T., Deichmann, N., Kissling, E., and Husen, S. (2009). Automatic S-wave picker for local earthquake tomography, *Bull. Seism. Soc. Am.,* **99**, 1906-1920.

Edwards, J. (1981). A brief description of the geology of Maryland: Maryland Geological Survey, Baltimore, Maryland.

Erickson, J.P., Carlson, D.K., Ortiz, A.M., Hutchenson, K.D., Owiesny, L.J., Kraft, G.D., Anderson, D.N., and Tinker, M.A. (2003a). Station correction uncertainty in multiple event location algorithms and the effect on error ellipses, *in* Proceedings of the 25th Seismic Research Review – Nuclear Explosion Monitoring; Building the Knowledge Base, 23-25 September 2003, Tucson, AZ.

Erickson, J.P., Ortiz, A.M., Tinker, M.A., Owiesny, L.J., Hutchenson, K.D., and Kraft, G.D. (2003b), Seismic location methods and capabilities: QTSI Technical Report QTSI_03/0001, December 2003.

Fisher, R.A. (1936). The use of multiple measurements in taxonomic problems, *Eugen.,* **7**, 179-188.

Gilbert, M. C. (1982). Geologic setting of the Eastern Wichita Mountains with a brief discussion of unresolved problems, *in* Gilbert, M.C. and R. N. Donovan, Eds., *Geology of the Eastern Wichita Mountains Southwestern Oklahoma*, Oklahoma Geological Survey, Guidebook 21, 1-30.

Hastie, T., Tibshirani, R., Friedman, J. (2009). *The elements of statistical learning (data mining, inference, and prediction)*, 2nd Edition, Springer, New York.

Hutchenson, K.D., R.B. Conner, L.B. Johnson, H.H Bennett, J.E. Simms, and D.E. Yule (2015). Evaluation and current results of the Seismic Acoustic Impact Monitoring Assessment (SAIMA) system, *J. Env. Eng. Geophys.*, **20**, No. 1, 89-100.

Hutchenson, K.D., Conner, R.B., Johnson, L.B., Bennett, H.H. Jr., Simms, J.E., and D.E. Yule (2013). Evaluation And Current Results of the Seismic Acoustic Impact Monitoring Assessment (SAIMA) System, presented at SAGEEP, Denver, CO, March, 2013.

Lay, T., and Wallace, T.C. (1995). *Modern Global Seismology*, Academic Press, San Diego.

McGinnis, L.D., Miller, S.F., Thompson, M.D., and McGinnis, M.G. (1992). Geophysical study of the Building 103 Dump, Aberdeen Proving Ground: Argonne National Laboratory, Argonne, Illinois.

Quantum Technology Sciences, Inc. (QTSI), (2015). Multi-Channel Product Qualification, Environmental Test Report, Summary of Results, QTSI Technical Report, unpublished.

Quantum Technology Sciences, Inc. (QTSI), (2013). Seismic-Acoustic Impact Monitoring System (SAIMA), QTSI Technical Report, W912HZ-11-C-0014.

Quantum Technology Sciences, Inc. (QTSI) (2012). SAIMA Demonstration and Data Collect, Analysis and Results, Ft. Sill, OK, 30 August 2012, Technical Report, Cocoa Beach, FL (unpublished).

Rost, S. and C. Thomas (2002). Array seismology: methods and applications, *Rev. of Geophys*., **40**, no. 3, 2.1-2.27.

SERDP and ESTCP (2007). Technical Exchange Meeting on DoD Operational Range Assessment and Management Approaches, October 2007.

Sharp, M.K., Butler, D.K., and Sjostrom, K.J. (1999). Integrated geophysical methods approach to subsurface geologic mapping utilizing high-resolution transient electromagnetic surveys: *J. Environmental and Engineering Geophysics*, **4**, 57-70.

Smart, E. and E.E. Flinn (1971). Fast frequency-wavenumber analysis and Fisher signal detection in real-time infrasonic array data processing, *Geophys. J. R. Astron. Soc*., **26**, 279-284.

Smith, S.W. (2002). *The Scientist and Engineer's Guide to Digital Signal Processing*, Newnes (online edition).

Schweitzer, J., Fyen, J., Mykkeltveit, S., Gibbons, S.J., Pirli, M., Kühn, D., and Kværna, T. (2012). Seismic Arrays, in Bormann, P. (Ed.), *New Manual of Seismological Observatory Practice* (NMSOP-2), IASPEI, GFZ German Research Centre for Geosciences, Potsdam; http://nmsop.gfz-potsdam.de; DOI: 10.2312/GFZ.NMSOP-2.

U.S. Army (2011). Military Installation Maps (MIM), Ft. Sill, OK, August 2011, Draft and Final.

USNDC (2010). United States National Data Center, Phase 3, Database Design Description (DBDD), QTSI, 30 November 2010.

VanDeMark, T.F., Johnson, L.B., Bennett, J., Simms, J.E., and Yule, D.E. (2009). Evaluation of seismic-acoustic analysis methods for a real-time UXO monitoring system: in Proceedings of the 22nd Symposium on the Application of Geophysics to Engineering and Environmental Problems (SAGEEP).

VanDeMark, T.F., Conner, R., Johnson, L.B., Bennett, J., Simms, J.E., and Yule, D.E. (2010). Technical overview of the Seismic-Acoustic Impact Monitoring Assessment (SAIMA) system: in Proceedings of the 23nd Symposium on the Application of Geophysics to Engineering and Environmental Problems (SAGEEP).

VanDeMark, T.F., Johnson, L.B., Pitarka, A., Bennett, H.H. Jr., Simms, J.E., and Yule, D.E. (2013). Evaluation of seismic-acoustic analysis methods for a real-time UXO monitoring system, *Jour. Env. Eng. Geophys.,* **18**(1), 71-85.

APPENDIX A POINTS OF CONTACT.

Points of contact for Quantum Technology Sciences, Inc. are contained in this section.

Name	Company	Email	Phone
Chris Bailey	QTSI	cbailey@qtsi.com	321.8680288x108
Ray Conner	QTSI	rconner@qtsi.com	321.8680288x116
Kevin Hutchenson, Ph.D.	QTSI	khutchenson@qtsi.com	321.868.0288x112

APPENDIX B FT. SILL, OK, FIRING LIST, OCTOBER 2016.

This appendix contains the firing list table from 13 October 2016 from Ft. Sill. The firing order, and HE and inert designations are provided.

Table 8. Shot Table, 13 October 2016, 155 mm and 105 mm.

Time (UTC)	Count	155 mm		105 mm		HE	Inert
		Paladin	777	A	B		
17:51:13	1			1		1	
17:55:07	2			2		1	
17:58:39	3			3		1	
18:03:37	4			4		1	
18:04:00	5			5		1	
18:04:07	6				1	1	
18:04:59	7				2	1	
18:18:07	8			6		1	
18:18:09	9				3	1	
18:18:32	10				4	1	
18:18:44	11			7		1	
18:32:33	12				5	1	
18:32:35	13			8		1	
18:33:02	14			9		1	
18:33:28	15				6	1	
18:51:47	16				7	1	
18:51:48	17			10		1	
18:52:12	18			11		1	
18:52:23	19				8	1	
18:52:32	20	1				1	
18:52:54	21		1			1	
19:02:56	22	2					1
19:04:26	23			12		1	
19:04:46	24			13		1	
19:14:04	25		2				1
19:24:25	26	8	3			1	
19:29:32	27		4			1	
19:33:48	28	3				1	
19:33:58	29		5			1	
19:35:02	30	4				1	
19:39:43	31		6			1	
19:50:14	32		7			1	
19:50:15	33	5				1	
19:51:04	34		8			1	
19:51:54	35	6				1	
20:09:05	36		9				1
20:09:09	37	7					1
20:09:55	38		10				1
20:10:47	39	8					1
20:11:14	40		11				1
20:11:53	41	9					1
20:28:21	42		12			1	
20:28:27	43	10				1	

Time (UTC)	Count	155 mm		105 mm		HE	Inert
		Paladin	777	A	B		
20:29:16	44		13			1	
20:29:30	45	11				1	
20:37:27	46		14				1
20:38:13	47		15				1
20:38:56	48	12					1
20:39:02	49		16				1
20:40:14	50	13					1
20:41:26	51	14					1
20:43:09	52				9	1	
20:47:48	53				10	1	
20:51:17	54				11	1	
20:54:55	55				12	1	
20:55:13	56				13	1	
20:55:41	57			14		1	
20:56:19	58			15		1	
21:03:56	59				14	1	
21:04:10	60			16		1	
21:04:25	61				15	1	
21:04:29	62			17		1	
21:18:28	63			18		1	
21:18:29	64				16	1	
21:18:47	65			19		1	
21:18:52	66				17	1	
21:19:00	67			20		1	
21:19:12	68				18	1	
21:19:15	69			21		1	
21:19:32	70			22		1	
21:19:44	71				19	1	
21:19:48	72			23		1	
21:20:07	73				20	1	
21:20:35	74				21	1	
21:33:57	75		17			1	
21:37:40	76			24		1	
21:38:13	77				22	1	
21:41:26	78		18			1	
21:42:03	79			25		1	
21:42:26	80		19			1	
21:43:01	81			26		1	
21:46:06	82	15				1	
21:48:03	83			27		1	
21:48:22	84			28		1	
21:48:23	85				23	1	
21:48:56	86			29		1	
21:49:05	87				24	1	
21:49:30	88				25	1	
21:52:33	89		20			1	
22:15:29	90	16				1	
22:17:11	91	17				1	
22:17:22	92	18				1	
22:18:46	93		21			1	
22:31:47	94	19					1

Time (UTC)	Count	155 mm		105 mm		HE	Inert
		Paladin	777	A	B		
22:32:31	95		22				1
22:33:21	96	20					1
22:33:23	97		23				1
22:34:18	98		24				1
22:35:25	99	21					1
22:48:33	100				26	1	
22:52:51	101				27	1	
22:56:59	102				28	1	
22:57:19	103				29	1	
22:57:41	104			30		1	
22:58:08	105			31		1	
23:08:58	106	22					1
23:10:18	107				30	1	
23:10:24	108				31	1	
23:10:37	109				32	1	
23:10:53	110			32		1	
23:14:46	111		25			1	
23:22:15	112				33	1	
23:22:21	113			33		1	
23:22:30	114				34	1	
23:22:40	115			34		1	
23:22:44	116				35	1	
23:23:00	117			35		1	
23:40:37	118	23				1	
23:41:20	119	24				1	
23:42:23	120	25				1	
23:43:02	121				36	1	
23:43:14	122			36		1	
23:43:15	123				37	1	
23:43:19	124	26				1	
23:43:34	125			37		1	
23:44:06	126	27				1	
23:45:08	127	28				1	
23:51:26	128			38		1	
23:51:26	129				38	1	
23:51:42	130				39	1	
23:51:52	131			39		1	
23:52:02	132				40	1	
23:52:17	133			40		1	
0:00:10	134	29					1
0:02:12	135	30					1
0:09:41	136	31				1	
0:10:19	137	32				1	
0:11:23	138	33				1	
0:12:09	139	34				1	
0:12:49	140	35				1	
0:13:39	141	36				1	
0:14:27	142	37				1	
	TOTALS:	**37**	**25**	**40**	**40**	**119**	**23**

APPENDIX C FT. SILL, EQUIPMENT ASSESSMENT, AUGUST 2014.

This appendix contains the contents of a memo assessing the state of the equipment deployed in August 2013.

++

ESTCP - SAIMA Assessment, Ft. Sill, OK (August 4-6, 2014)

Objective

Assess the SAIMA system currently deployed at Ft Sill. Determine the number of working nodes, sensors, radios, battery power, and solar panels. Retrieve recorded data from nodes, measure sensor performance, radio performance, and power condition. Identify possible future array sites and review range schedules for follow-on data collects.

Equipment Status – Field Notes

Site #1 – SMART 2

Node box lights on, SBC good – All channels look good.
Recorded data: SDD – 84%, Flash Drive – 100% recorded CD11 and log data.
Radio – good
Batteries – charged (12.51v, 12.54v)
Solar panel and controller - good
Directional Antenna – good
GPS – chewed cable
Sensors 3, 5, 8 – open circuit (or bad cables)
Sensor 4 - short
Sensors 1, 2, 6, 7 – good

Site #2 – SMART 3

Node box lights on, SBC good – All channels look good.
Recorded data: SDD – 100%, Flash Drive – 100% recorded CD11 and log data.
Radio – good
Batteries – charged (12.93v, 12.93v)
Solar panel and controller - good
Dipole Antenna – tip chewed off
GPS – chewed cable
Sensors 3, 5 – open circuit (or bad cables)
Sensor 4 – no cable or connector
Sensors 1, 2, 6-8 – good

Site #3 – SMART 4

Node box lights on, SBC good – channel 5 has DC offset and data glitches (low amplitude). All other channels look good.
Recorded data: SDD – 100%, Flash Drive – 100% recorded CD11 and log data.
Radio – bad (SN: W11389607)
Batteries – charged (13.15v, 13.1v)
Solar panel and controller - good
Directional Antenna – good, chewed Ethernet cable
GPS – chewed cable
Sensors 2 & 8 – open circuit (or bad cables)
Sensors 1, 3-7 – good

Site #4 – SMART 5

Node box lights on, SBC good – all channels look good.
Recorded data: SDD 81%, Flash Drive – 100% recorded CD11 and log data.
Radio – good
Batteries – charged (12.9v, 12.86)
Solar panel and controller – good
Directional Antenna – good
GPS – good
Sensors 1, 2, 8 – open circuit (or bad cables)
Sensor 4 – short ? (70+ mA)
Sensors 3, 5-7 – good

Site #5 – SMART 6

Node box lights off, SBC good – channels 4, 5, 8 have DC offset and data glitches (low amplitude). All other channels look good.
Recorded data: SDD – 100%, Flash Drive – 100% recorded CD11 and log data.
Radio – good
Batteries – dead (5.31v, 5.31v)
Solar panel – good, controller – bad
Directional Antenna – good
GPS – good
Sensors 1, 5, 6, 7 – open circuit (or bad cables)
Sensors 2-4, 8 – good

Trigger – SMART 1

Node box lights off, SBC good – Trigger channel look good.
Recorded data: SDD – ? %, Flash Drive – ? % recorded CD11 and log data.
Radio – good
Batteries – dead (1.81v, 1.82v)
Solar panel – good, controller – bad
Dipole Antenna – good
GPS – cable chewed
Sensor 1 – good

Success Criteria

The system can be restored to operational state for follow-on data collections. (YES)

++